

**COMBINING LIDAR, MULTI-SPECTRAL IMAGERY AND GIS  
TO ASSESS RIPARIAN AREA CONDITIONS**

A Thesis  
Presented to  
The Faculty of  
Western Washington University

In Partial Fulfillment  
Of the Requirements of the Degree  
Master of Science

by  
Kari A. Secret  
February 2007

# Table of Contents

Abstract .....	iv
Acknowledgements .....	v
List of Tables .....	vii
List of Figures .....	viii
1.0 Introduction .....	1
1.1 Introduction .....	1
1.2 Research Objectives .....	3
2.0 Background .....	5
2.1 Shade Production .....	5
2.2 Large Woody Debris Recruitment .....	6
2.3 Study Area .....	7
3.0 Methods .....	10
3.1 Data Sources .....	10
3.2 Extracting Vegetation .....	13
3.3 Generating Forest Type .....	16
3.4 Model Overview .....	19
3.5 LWD Model Component .....	22
3.6 Shade Model Component .....	30
3.7 Forest Buffer Characteristics Model Component .....	41
4.0 Results and Discussion.....	44
4.1 Forest Type Accuracy Assessment .....	44
4.2 Model Results Accuracy Assessment .....	45
4.3 LWD Potential .....	46
4.4 Shade Potential .....	49
4.5 Secondary Riparian Area Characteristics .....	54
4.6 Ranking Riparian Conditions .....	55
4.7 Future Model Improvements .....	61
5.0 Conclusions .....	63
Literature Cited .....	65

## Abstract

I used a combination of lidar data, multi-spectral imagery and GIS hydrology data for the Fir Island area of Skagit County, Washington to develop a GIS model that evaluates and maps hydrology features based on two key riparian area characteristics important for supporting healthy salmon habitat: large woody debris (LWD) delivery and shade. The model consists of custom applications written in Visual Basic for Applications that run within ESRI's ArcGIS software.

The lidar data and multi-spectral imagery provide input to the model regarding the location of riparian forest and its approximate height throughout the study area.

The LWD and shade models rank all 10-meter hydrology line segments in the study area relative to the best in the study area. The LWD model ranked 78.6% of the study area with the poorest value of 1, while only 0.1% of the study area received the highest ranking value of 10. The potential shade model ranked 88% of the study area with the poorest value of 1, while only 2.8% received the highest shade ranking value of 10. The study area's land use is primarily agricultural in nature so the high percentage of poorer ranked sites and low percentage of highest ranked sites was not unexpected. The model additionally quantified the presence and width of forested riparian buffers as well as information about the forest composition within them. This information was combined with the LWD and shade potential results to apply an overall riparian condition ranking to all hydrology features, subdivided into 10-meter segments, within the study area in order to identify and map potential restoration and preservation sites.

## Acknowledgments

I would like to acknowledge all the people who have contributed to the successful completion of this work.

My deepest thanks go to my thesis advisor, Dr. David Wallin, for his invaluable advice, direction, and patience as I floundered my way through this process. I cannot imagine having completed this work without his guidance.

Thanks also to Dr. Michael Medler, for his insights during the early stages of the development of the research goals and for his helpful comments on the text.

Many thanks to Dr. Joshua Greenburg, whose experience, advice and wonderful sense of humor has been such a help to me throughout this process.

Thanks also to Geoffrey Almvig, my supervisor, for going out of his way to support me throughout this endeavor.

My sincerest thanks to my parents, Nicholas and Pamela Secrest, who have believed in me, sacrificed for me and always made my education one of their top priorities. They have provided me with much support, an incredible willingness to accept and always an eagerness to love. I hope this work makes them proud.

Last, but certainly not least, I must acknowledge with tremendous thanks and love my partner, Deanna Randall. Through her love, support, neverending patience and unfaltering belief in me, I've been able to complete this journey. I could never have done it without her so this work, and my life, is dedicated to her.

## List of Tables

Table 3.1 Spectral ranges for each band of theDAIS-1 Space Imaging sensor .....	12
Table 4.6 Forest type layer accuracy assessment error matrix from 35 field visited sites .....	45
Table 4.2 LWD rankings 1-10 assigned according to LWD index values .....	47
Table 4.3 Shade rankings 1-10 assigned according to Shade index values.....	49
Table 4.4 Forest buffer width rankings 1-10 assigned according to the percentage of the buffer that is forested located adjacent to the RCS .....	54
Table 4.5 Percent buffer conifer-dominant rankings 1-10 assigned according to the percentage of the buffer that consists of conifer-dominant forest .....	55
Table 4.6 LWD index and shade index were combined to create a primary combined rank (PCR) value for each RCS .....	56

## List of Figures

Figure 2.1 Study area map and vicinity .....	9
Figure 3.1 DAIS multi-spectral color composite image with a spatial resolution of 1 meter .....	11
Figure 3.2 GIS hydrology layer digitized from the DAIS multi-spectral image .....	13
Figure 3.3 Vegetation map of the study area created by classification of the 1-meter DAIS image (August 2001) using Feature Analyst software .....	14
Figure 3.4 4-meter bare earth elevation grid created from lidar last return data points collected in April 2002 .....	16
Figure 3.5 4-meter first returns grid created from first return lidar data points collected in April 2002 .....	17
Figure 3.6 4-meter surface feature height grid generated by calculating the difference between lidar-based surface feature elevation and bare earth elevation grids .....	18
Figure 3.7 Forest type map showing vegetated areas (extracted from 1-meter multi-spectral imagery) with a canopy height greater than or equal to 3 meters .....	19
Figure 3.8 Methodology flow diagram .....	21
Figure 3.9 Probability space of a given tree fall whose radius is equal to tree height .....	23
Figure 3.10 Simulated tree fall using a 10-degree polar array of lines equal to tree height .....	24
Figure 3.11 Functional probability space defined as the area common to both the tree height radius circle and the stream edge .....	24
Figure 3.12 Potential LWD pieces .....	25
Figure 3.13 Study area example of candidate tree fall arrays created using line lengths equal to lidar-generated height values .....	26
Figure 3.14 A second set of potential LWD pieces are generated using maximum study area trees .....	27

Figure 3.15 Infrared view of the study area where MSAHT values were identified using the forest type layer overlaid with the surface feature height grid to identify the tallest conifer-dominant (64.9m) and deciduous-dominant (53.6m) tree heights within the study area .....	29
Figure 3.16 Sun position and tree height are used to estimate shadows .....	31
Figure 3.17 Top-down view of a tree located at M and sun azimuth of 208 degrees .....	33
Figure 3.18 Right triangle KLM .....	34
Figure 3.19 Side MN of right triangle MNO represents the shadow cast by a tree located at point M .....	35
Figure 3.20 Length MO represents change in Y-direction and ON represents the change in X-direction for the shadow's endpoint .....	36
Figure 3.21 Study area example of candidate tree shadows generated using lidar-generated tree height values .....	38
Figure 3.22 Potential shadows generated using MSAHT values .....	39
Figure 3.23 Right and left 33-meter length transects are placed at the endpoint of each RCS .....	41
Figure 3.24 Transects are subdivided into smaller pieces by overlaying the forest type layer .....	42
Figure 4.1 Map showing LWD ranking of RCSs where lower values indicate decreased potential LWD contribution and larger values indicate increased potential LWD contribution .....	48
Figure 4.2 Map showing RCS shade rankings where lower values indicate decreased shade potential and larger values indicate increased shade potential .....	50
Figure 4.3 Shading bias is observed here for the portion of this stream oriented in a east-west direction over the portion of the stream having a more north-south orientation .....	51
Figure 4.4 LWD Index is not affected by the bias as Shade Index due to potential LWD polar arrays that cover 360-degrees .....	52
Figure 4.5 Overhanging coniferous and deciduous forest canopy vegetation .....	53

Figure 4.6 Map of PCR values for each RCS within the study area ..... 57

Figure 4.7 Potential preservation and restoration sites for which field visits are recommended ..... 58

Figure 4.8 A series of RCSs are identified here as potential preservation sites with green triangles overlaid to identify them. Conifer-dominant forest patches in dark green and deciduous-dominant forest patches shown in light green. RCSs along each side of the stream are shown as blue 10-meter segments with arrows signifying each segment’s endpoint ..... 60

Figure 4.9 Two RCSs are identified here as potential restoration sites with red points overlaid to identify them. Conifer-dominant forest patches in dark green and deciduous-dominant forest patches shown in light green. RCSs along each side of the stream are shown as blue 10-meter segments with arrows signifying each segment’s endpoint ..... 61

# 1.0 Introduction

## 1.1 Introduction

In response to the listings of Pacific Northwest salmon under the Endangered Species Act, riparian areas and the aquatic habitat they support have been the focus of extensive preservation and restoration efforts. Throughout the Puget Sound region, aquatic habitat preservation and restoration activities within riparian areas have been conducted by non-profit organizations, federal, state, tribal and local government agencies.

In order to successfully manage riparian areas for this purpose, two questions emerge: “What critical functions do riparian areas provide for aquatic habitat?” and “How can riparian area functionality be assessed and monitored?” It is generally accepted that high-functioning riparian areas provide the following vital ecosystem functions:

- 1) Large Woody Debris (LWD) Recruitment – trees, large branches, and root wads that fall into a stream create refuge pools for salmon that allow them to forage for food, save energy, and gain protection from predators (Bisson et al. 1987, Bryant 1983, Naiman et al. 1982, Sedell et al. 1988, Swanson et al. 1976).
- 2) Shade Production – riparian vegetation provides shade that maintains low stream temperatures which are vital for salmonids (Beschta et al. 1987, Brown 1969, Brown and Krygier 1970, Gregory et al. 1991).
- 3) Sediment Reduction – riparian vegetation can act as a filter and thereby reduce transfer of pollutants such as sediment, nutrients, road salt and agricultural chemicals from upland areas to adjacent watercourses (Duncan et al. 1987, Gregory et al. 1991, Sovell et al. 2000).

- 4) Particulate Organic Matter (POM) Recruitment – riparian vegetation provides detrital organic matter such as leaves, cones and needle litter that are important in aquatic food chains (Endreny 2002, Gregory et al. 1991).
- 5) Streambank Stabilization – plant roots of riparian vegetation slow down erosion along stream banks and help maintain floodplain integrity (Lamberti et al. 1991, Murgatroyd and Ternan 1983).
- 6) Microclimate – riparian vegetation plays an important part in maintaining the soil moisture, humidity levels, air temperature and solar radiation levels, etc. that make up the unique microclimate present in riparian areas (Castelle et al. 1994, Duncan et al. 1987, Endreny 2002, Turner et al. 2001, Young 2000).

Of these, LWD recruitment and shade production are particularly important to providing and maintaining suitable salmon habitat (Beechie and Sibley 1997, Brown and Krygier 1970, Bryant 1983, Castelle et al. 1994, King County 1997).

During the last 150 years, riparian forests in the Puget Sound region have been dramatically degraded by the cumulative impacts of a wide variety of anthropogenic factors including logging, agriculture and urban development. Clearing or harvesting trees in riparian areas along with nearby road construction can impact ecosystem functions within riparian areas, resulting in large losses and degradation of aquatic habitat (Beechie 1998, Beechie and Sibley 1997, Brown and Krygier 1970, Duncan 1987). Due to these varied land use applications and given the history of natural resource exploitation within this region, managing and restoring riparian forests will require a diversity of approaches.

Vannote et al. (1980) presented the “River Continuum Concept” that describes the presence of a gradient that exists between a river system’s headwaters and its mouth such

that downstream biological communities are adapted to capitalize on upstream processing inefficiencies. With this concept in mind, it is important to recognize that upstream riparian forests may have different requirements regarding LWD recruitment and shade production than those in lower, more developed areas within a given watershed.

Given the uniqueness of each riparian forest and the needs of various organizations to assess and monitor their function for aquatic habitat purposes, it is necessary to develop tools that can help analyze and map riparian forest conditions and function. A geographic information system (GIS) can describe riparian forest conditions at a site-specific scale, but also on a watershed and/or regional-scale context when evaluating a given site. For this reason, GIS is a valuable tool when used for objectively assessing and monitoring aquatic habitat for the purpose of managing preservation and restoration activities. Previous research has shown that GIS models are particularly well-suited for gathering and analyzing spatial information regarding aquatic habitat conditions. GIS models have already been employed as valuable tools for salmon habitat planning at both the regional and watershed levels (Hyatt et al. 2004, Lunetta et al. 1997, Waldo 2003). However, there is a need for further development of GIS models that can be used to aid in the assessment and monitoring of riparian forest functionality.

### 1.2 Research Objectives

The purpose of this research is to develop a methodology to objectively evaluate two key characteristics of riparian forests that are essential to providing and maintaining suitable aquatic habitat: LWD recruitment and shade production. To achieve this goal, I will develop a GIS model that uses remotely sensed data. The model will provide planners and

decision-makers with an objective method of selecting, managing and monitoring potential habitat restoration and/or preservation sites that directly impact salmon habitat.

This study uses vector data, multi-spectral imagery and lidar data within the framework of a GIS to provide information about the location and functionality of riparian forests within the study area. The model results in two outputs:

- 1) A GIS dataset consisting of hydrology line and polygon features containing attributes about the condition of the adjacent riparian forest within the study area including potential LWD recruitment and shade production potential along with other riparian area attributes such as riparian forest composition, forest buffer width, and forest canopy height.
- 2) A map depicting potential LWD recruitment and shade production potential at a site-specific scale that can be used to identify and rank potential riparian preservation and restoration sites.

## 2.0 Background

### 2.1 Shade Production

Research has shown that while many factors influence stream temperature including solar insolation or radiation, groundwater inputs, ambient air temperature, humidity, and elevation (Adams and Sullivan 1990, Berg et al. 2002, Brown 1969, Brown and Krygier 1970, Parkyn et al 2003), solar radiation stands out as a key environmental factor governing stream temperature change. Direct solar radiation can be absorbed, reflected, or transmitted and arrives at the earth's surface in virtually parallel rays (Campbell 1996). Since the position of the sun in the sky is a function of latitude, time of year and time of day, the azimuth and the altitude of the sun can be calculated (Cross 2002). The shade potential model used in this research combines sun azimuth and altitude information along with riparian forest canopy height data and the forest's proximity to a watercourse in order to estimate the potential shade production provided by a riparian forest to its adjacent watercourse.

Stream temperatures are influenced by a variety of factors. Elevation moderates a stream's daily diurnal and seasonal temperature cycles and a stream's temperatures tend to increase downstream from its headwaters towards the ocean (Sullivan et al. 1990, Zwieniecki and Newton 1999). Although research has demonstrated that daily mean stream temperatures consistently remain very close to daily mean air temperatures, variations around the daily mean temperature are highly influenced by sun exposure (Adams and Sullivan 1990). Stream temperatures are highest during the summer and the compounding factors of increased solar insolation, higher air temperature and decreased stream flows appear to be major influences on stream temperature (Beschta et al. 1987). Riparian forests

control the amount of direct solar radiation that reaches a watercourse. Therefore, the presence of an intact riparian forest results in lower diurnal stream temperature fluctuations (Barton et al. 1985, Brazier and Brown 1973, Brown and Krygier 1970).

## 2.2 Large Woody Debris Recruitment

Riparian areas are the chief suppliers of LWD to a given watercourse. LWD, including entire trees, root wads and large branches, is a key component of stream system structure (Bisson et al. 1987, Bryant 1983, Naiman et al. 1982, Swanson et al. 1976). Stream channel complexity is increased when LWD redirects and impedes stream flow thereby forming pools and eddies that are important for creating and maintaining fish habitat (Beechie and Sibley 1997, Bryant 1983). Additionally, recruited LWD provides stream nutrients (Sedell et al. 1988), sediment confinement (Sedell et al. 1988), alteration of stream gradient (Bilby and Ward 1989), and cover from predators and protection during high stream flows (Washington Forest Practices Board 1997).

For much of the past 100 years, the function and significance of LWD within the riparian area ecosystem, and more specifically aquatic habitat, have been commonly misconstrued. LWD was historically viewed as harmful to the environmental health of a waterway. For this reason, forest management commonly included the removal of LWD from fish-bearing streams after logging operations (Bisson et al. 1987). Research conducted over the last 25 years has demonstrated that LWD plays a vital role in maintaining the function and structure of aquatic habitat. (Beechie and Sibley 1997, Bisson et al. 1987, Bryant 1983).

LWD recruitment occurs via a variety of biological and physical processes.

Biological occurrences that produce tree fall include windthrow, insect-induced and disease-induced mortality. Physical processes include debris avalanches, redistribution from upstream locations, mass soil movements, and failure of stream banks due to undercutting (Keller and Swanson 1979, Swanson et al. 1976). LWD is most frequently contributed via windthrow, stream bank failure, and mortality due to natural processes (Bisson et al. 1987, Bryant 1983, Swanson et al. 1976). However, even though debris torrents occur less frequently, they can contribute large quantities of LWD (Lamberti et al. 1991).

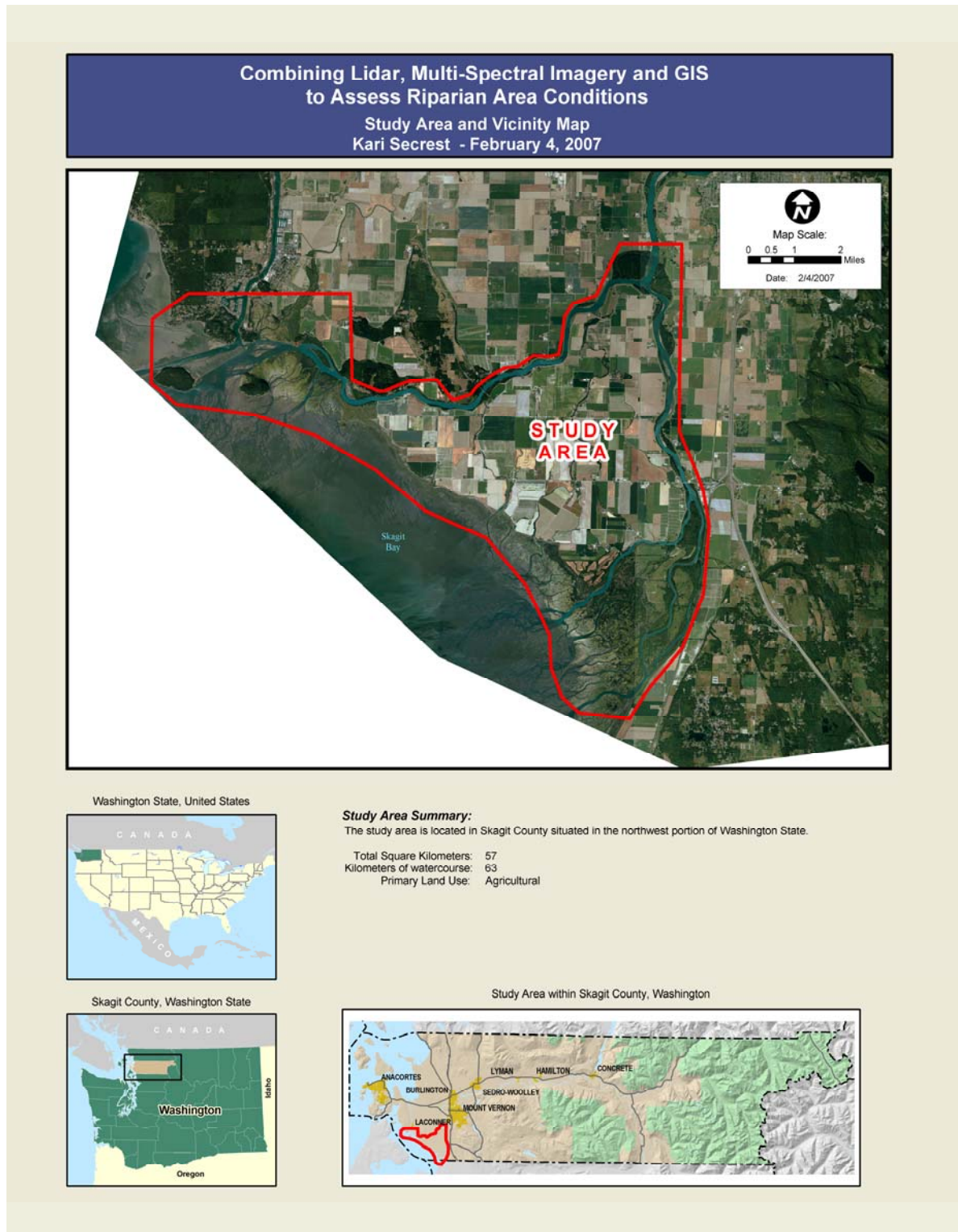
The size distribution of individual trees is an important factor when considering the effectiveness of LWD once it has been deposited in-stream. Research has shown a relationship between stream channel width and the size of LWD that is able to form the pools necessary to create and maintain quality aquatic habitat (Beechie 1998, Beechie and Sibley 1997, Bilby and Ward 1989, WFPB 1997). As stream channel width increases, the minimum functional LWD size must increase accordingly in order for pool forming to occur (Beechie 1998, Beechie and Sibley 1997, Bilby and Ward 1989, WFPB 1997).

### 2.3 Study Area

In recent decades, the Skagit River delta has been identified as important habitat for both juvenile salmon and wintering waterfowl. At the turn of the last century, like much of the Puget Sound lowlands, a large portion of the Skagit River delta was drained and diked for agricultural purposes. Skagit County's approach to salmon protection has been ongoing since 1996 when it adopted its first Critical Areas Ordinance (CAO) in order to comply with the state of Washington's Growth Management Act (Skagit County, 2003). Critical areas are defined by the Skagit County Planning Department as wetlands, aquifer recharge areas,

frequently flooded areas, geologically hazardous areas, and fish and wildlife habitat conservation areas. The study area for this research is located in the southwestern coastal region of Skagit County, Washington (Figure 2.1) and covers approximately 57-km<sup>2</sup>. The area includes approximately 403 km of watercourse, much of which is buffered with riparian forest of varying widths. The land-use within the study area is primarily agricultural.

Figure 2.1 Study area map.



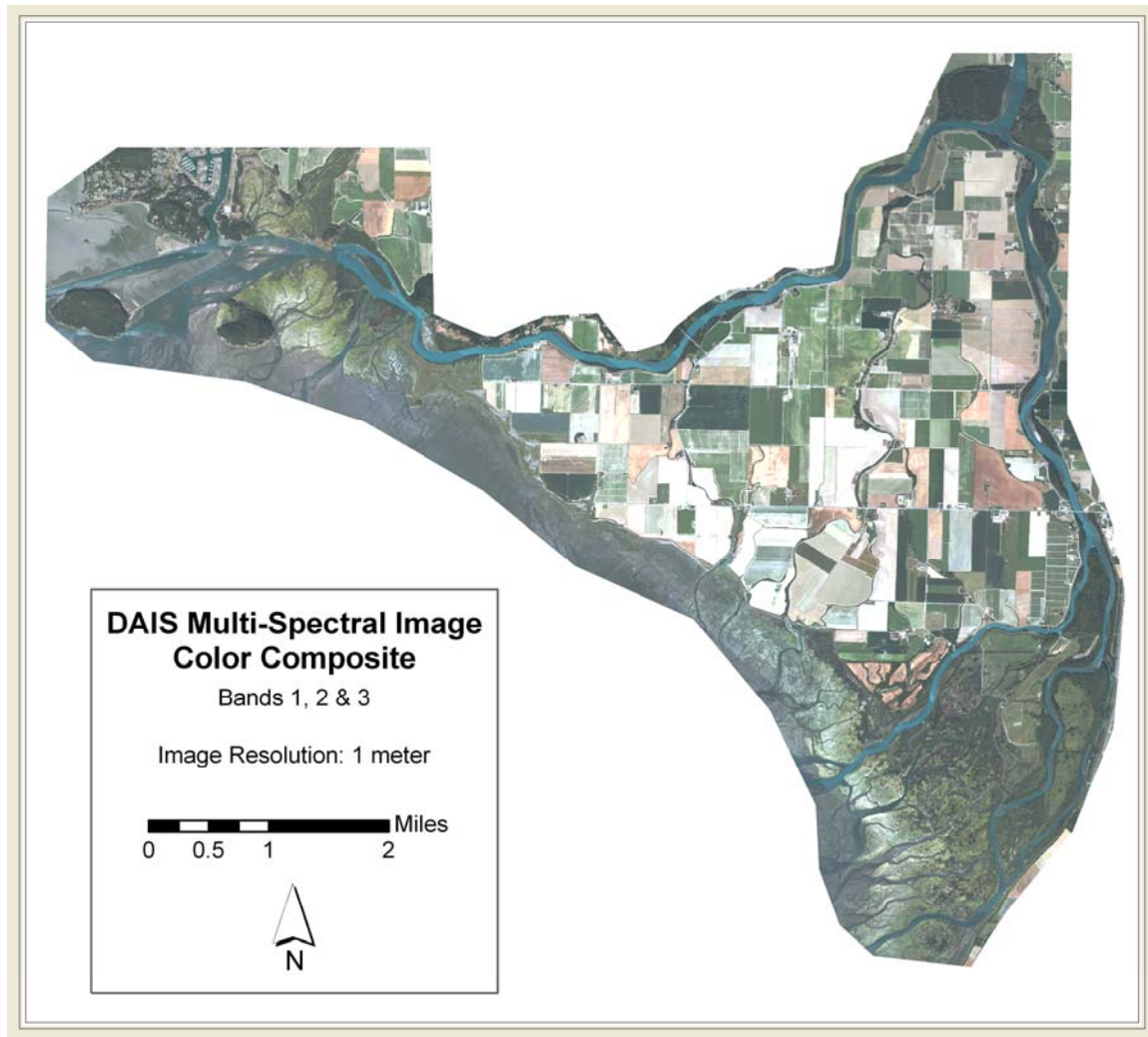
## 3.0 Methods

### 3.1 Data Sources

I used three primary data sources for the study area that include Lidar data, multi-spectral imagery and hydrology data. Lidar data was acquired for the study area from an airborne platform (Spencer B. Gross, Portland, OR for Skagit Systems Cooperative, LaConner, Washington) in April 2002 using the Aeroscan lidar system. This system has a small average footprint diameter of 60 cm and records multiple geolocated vertical returns using an onboard GPS system coupled with an inertial measurement unit. Acquisition occurred from an altitude of 7500 feet and the system emits 15,000 pulses per second with a cross-track spacing of 4.4 meters and along-track post (point density) spacing at 3.4 meters providing an average spacing of 4 meters. The vendor stated a horizontal accuracy of 30 centimeters and vertical accuracy of 15 centimeters for both first and last return point datasets. An additional vertical accuracy assessment was performed by Skagit Systems Cooperative. Ground elevations, low emergent vegetation, cattail and shrub heights were collected via GPS. They reported a 12 centimeter variance between the field-collected elevations and lidar data bare earth elevations. A 15 centimeter variance was calculated for both the low emergent vegetation and cattails. The variance between the field-collected shrub elevations and the lidar data points was 58 cm which may indicate the accuracy of the lidar data is diminished as canopy height increases.

Multi-spectral imagery, having a spatial resolution of 1 meter, was also used in conjunction with the lidar data (Figure 3.1).

Figure 3.1 DAIS multi-spectral color composite image with a spatial resolution of 1 meter. The image was acquired during the 1<sup>st</sup> week of August 2001.



This imagery was acquired via the Digital Airborne Imaging System (DAIS-1) during the first week of August in 2001. The DAIS-1 sensor is an airborne sensor owned and operated by Space Imaging, Inc. and is radiometrically calibrated and corrected for systematic distortions including optical vignetting, lens distortion, detector non-uniformity, and dark noise. The sensor's bands 1 (blue), 2 (green), 3 (red) and 4 (near infrared) are similar to the Landsat ETM bands 1 through 4 (Table 3.1).

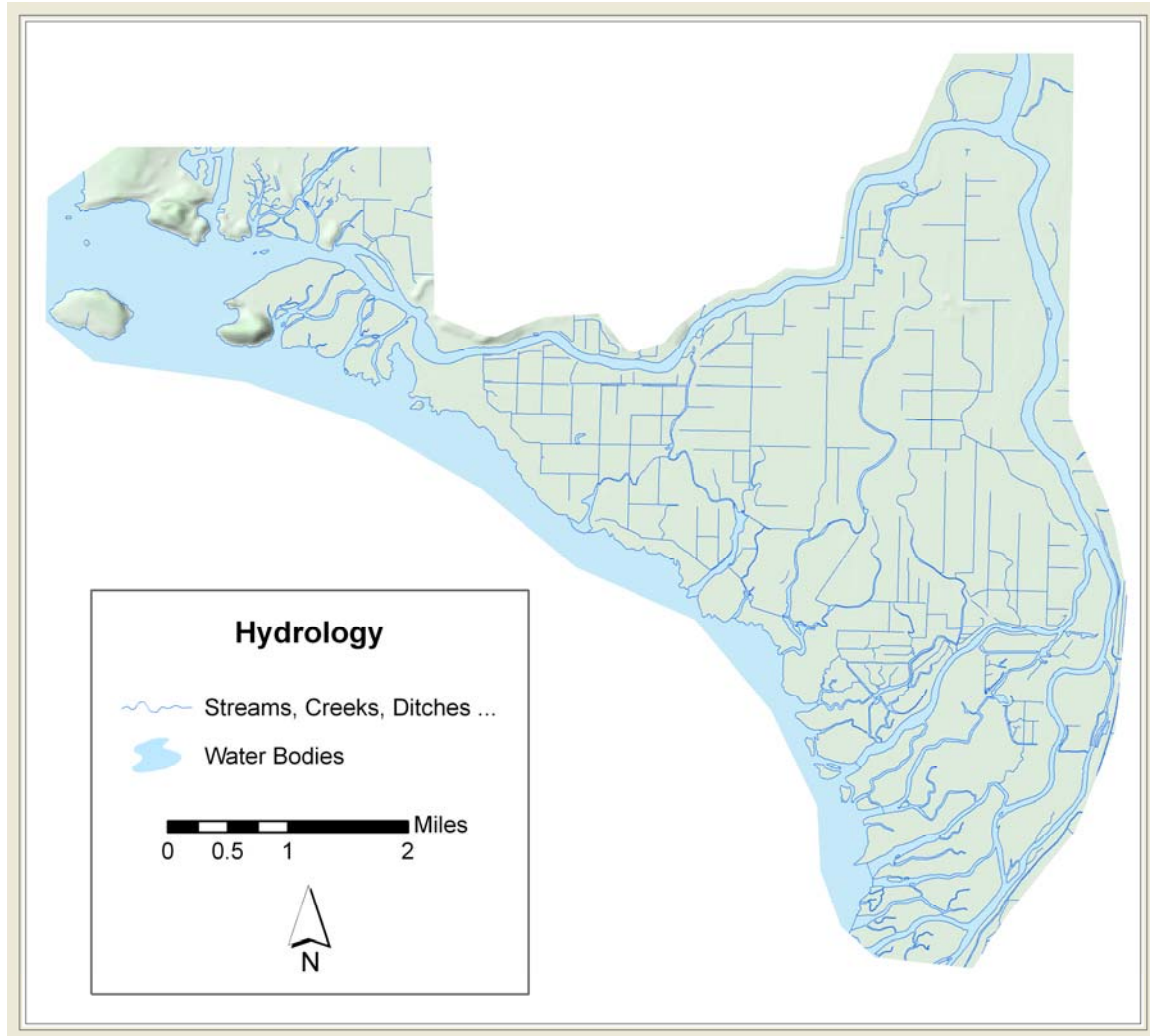
Table 3.1 Spectral ranges for each band of theDAIS-1 Space Imaging sensor. (Space Imaging, Inc., 2001)

<b>Band</b>	<b>Spectral Range</b>
Band 1	450 - 530 nm (blue)
Band 2	520 - 610 nm (green)
Band 3	640 - 720 nm (red)
Band 4	770 - 880 nm (NIR)

The imagery has a radiometric resolution of 12-bit, stored as 16-bit data in four bands, and is band-to-band co-registered as well as georectified. (Space Imaging, Inc. 2001)

The hydrology GIS dataset (Figure 3.2) used in this research was provided by Skagit County. This dataset was developed by the county to provide a hydrology dataset that improved upon the Washington State Department of Natural Resources (WADNR) hydrology dataset in terms of watercourse location. The hydrology data layer was generated manually by evaluating and digitizing each watercourse as it compares to the multi-spectral DAIS imagery also used in this research. Wherever necessary, watercourse features were re-digitized per the imagery. In some cases, actual field assessments were made to verify the accuracy of the digitized watercourse features. The entire study area consists of approximately 403 kilometers of hydrologic line features that were divided into a GIS data layer consisting of 40,341 10-meter segment lengths. For the purpose of this study, each 10-meter segment is known as a riparian condition segment (RCS).

Figure 3.2 GIS hydrology layer digitized from the DAIS multi-spectral image.

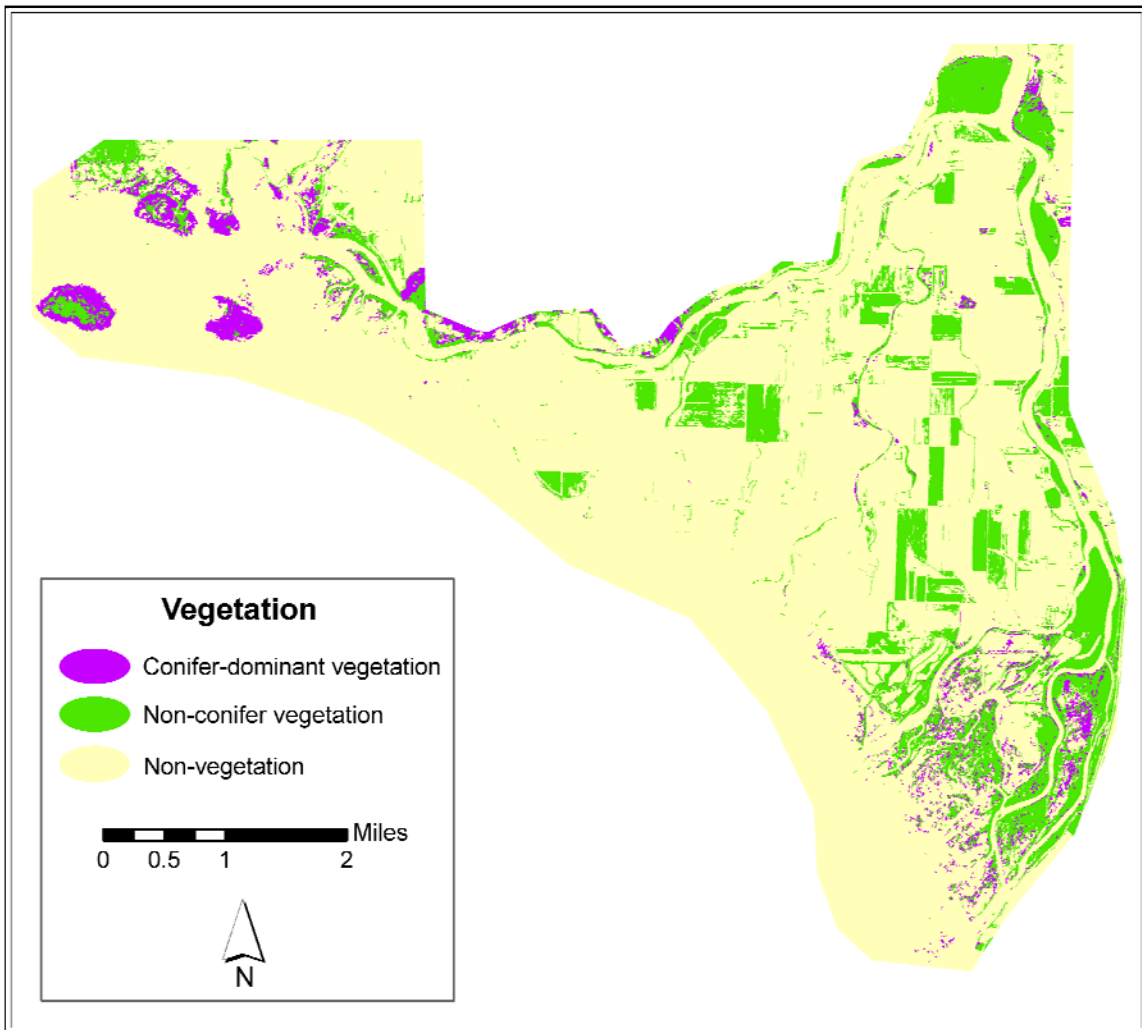


### 3.2 Extracting Vegetation

A vegetation layer was created by classifying the DAIS imagery using VLS Inc.'s Feature Analyst software. This software performs feature recognition and extraction by separating the image pixels into classes using not only spectral-radiometric differences, but spatial context, texture and pattern as well. Traditional image processing techniques incorporate only the spectral signature to separate features within an image. The Feature

Analyst software incorporates these processes into statistical and machine learning algorithms. The user inputs a set of training examples from which the software detects the spectral, textural and pattern differences and uses them to classify the image. The end result was a data layer comprised of polygons categorized as conifer-dominant vegetation, non-conifer vegetation and non-vegetated areas (Figure 3.3).

Figure 3.3 Vegetation map of the study area created by classification of the 1-meter DAIS image (August 2001) using Feature Analyst software. Classification is based on spectral information, spatial context, texture and pattern.



I selected these classes based on the 1997 Washington Forest Practices Boards protocol

which states:

"Although the analyst could expend much effort pursuing detailed information, the main objective is to identify riparian areas that naturally supported either conifer-dominated, hardwood-dominated forests or non-forest vegetation that provided low levels of woody debris and/or shade." (WFPB 1997, p. D-13)

### 3.3 Generating Forest Type

In order to extract forested areas from the vegetation layer, a general surface feature height raster data layer was required. To create this raster dataset, two input lidar grids were required: a bare earth elevation grid and a first returns elevation grid representing the tops of all surfaces (i.e. rooftops, roads, tree canopy, etc.) I created both 4-meter raster layers from the raw lidar point data provided to me by Skagit Systems Cooperative. The bare earth lidar points were used to create the 4-meter bare earth grid (Figure 3.4) and the first return lidar points were used to create the 4-meter first returns grid (Figure 3.5).

Figure 3.4 4-meter bare earth elevation grid created from lidar last return data points collected in April 2002.

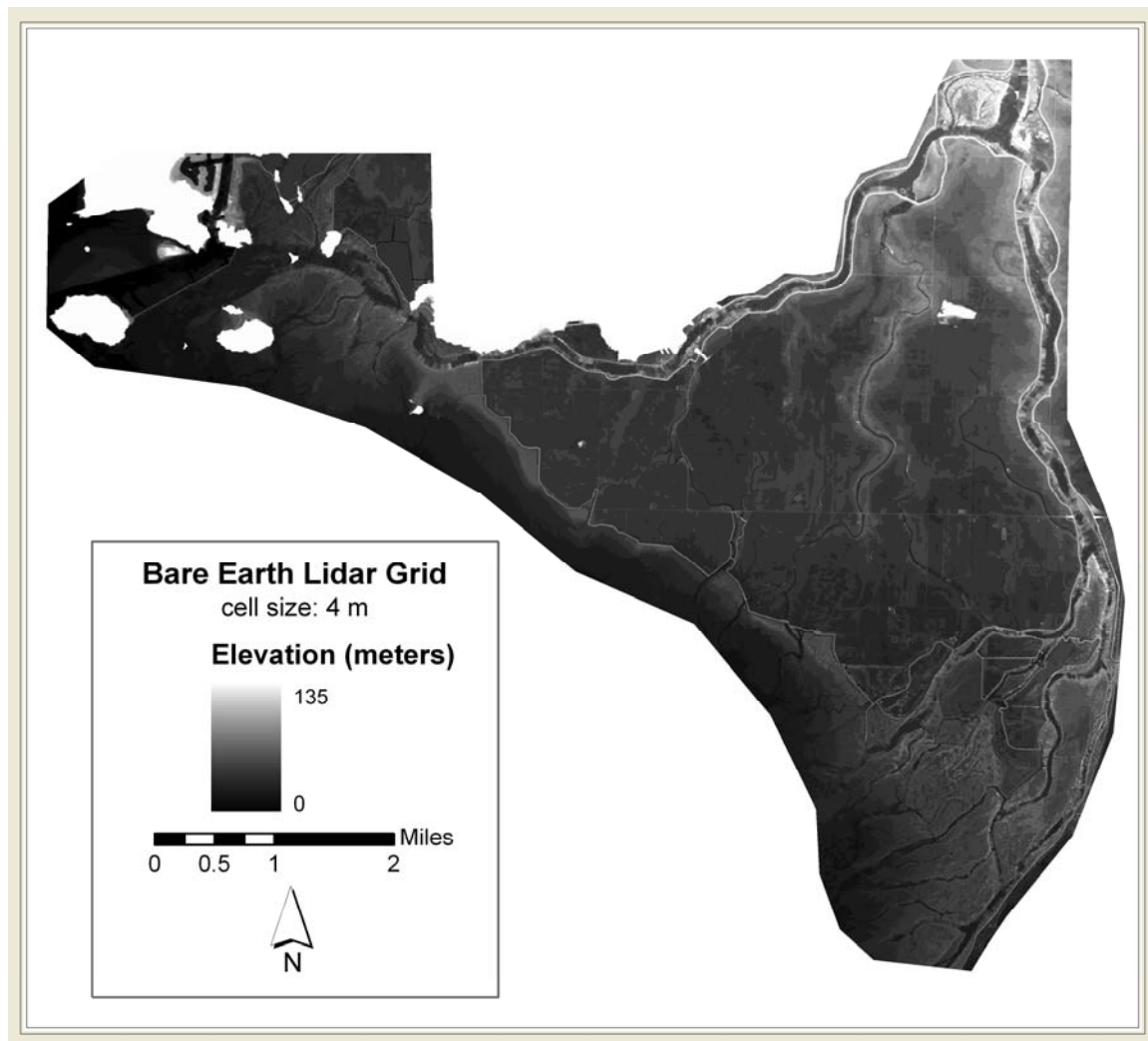
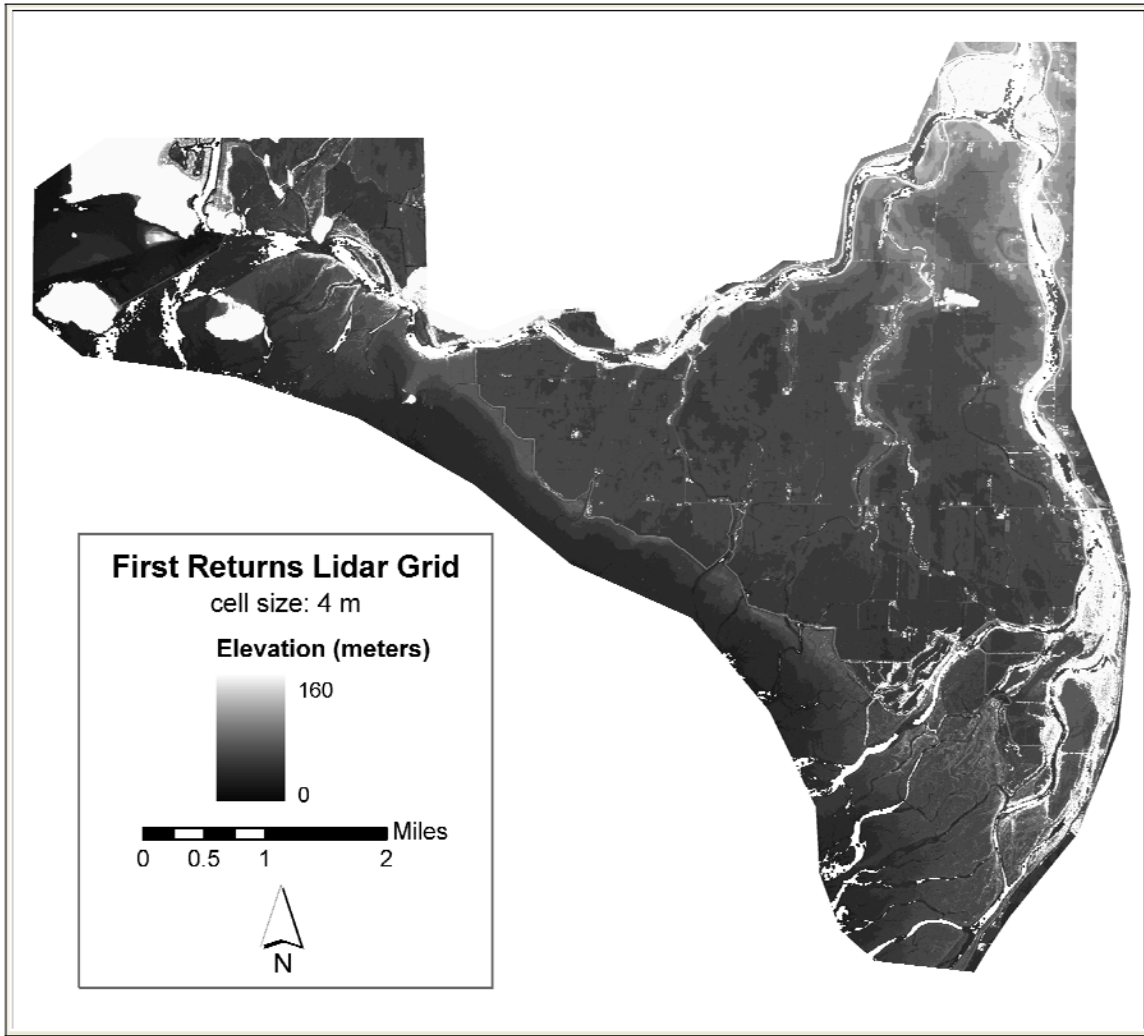
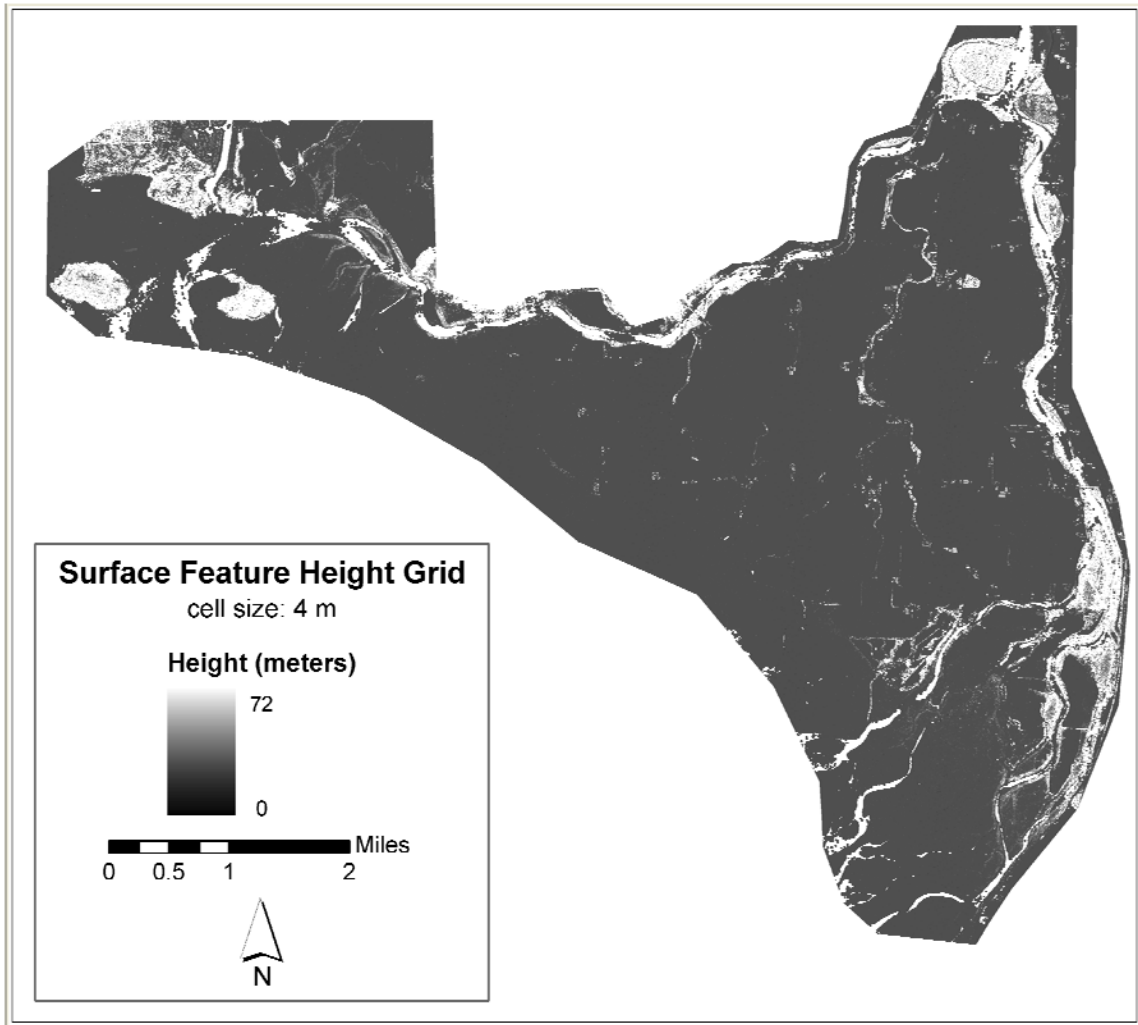


Figure 3.5 4-meter first returns grid created from first return lidar data points collected in April 2002.



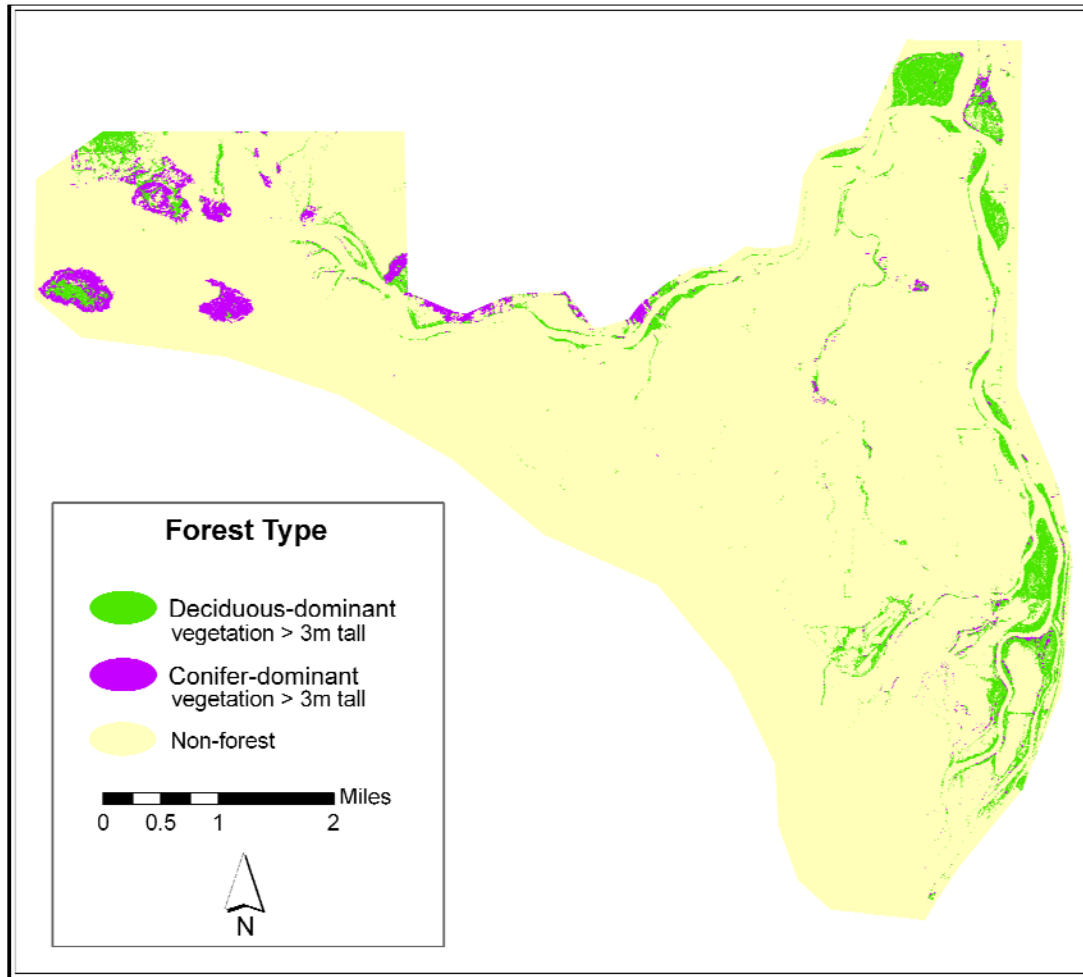
From these two grids, I created a 4-meter surface feature height grid (Figure 3.6) by subtracting the bare earth return grid values from the first return grid values.

Figure 3.6 4-meter surface feature height grid generated by calculating the difference between lidar-based surface feature elevation and bare earth elevation grids.



The forest type layer was created by overlaying the surface feature height grid with the vegetation layer and filtering out all vegetated areas with a canopy height value less than or equal to 3 meters such as grasslands and shrubs. Thus, the forest type layer shown in Figure 3.7 is defined for this study as the conifer-dominant and deciduous-dominant vegetation greater than 3 meters in height.

Figure 3.7 Forest type map showing vegetated areas (extracted from 1-meter multi-spectral imagery) with a canopy height greater than or equal to 3 meters.

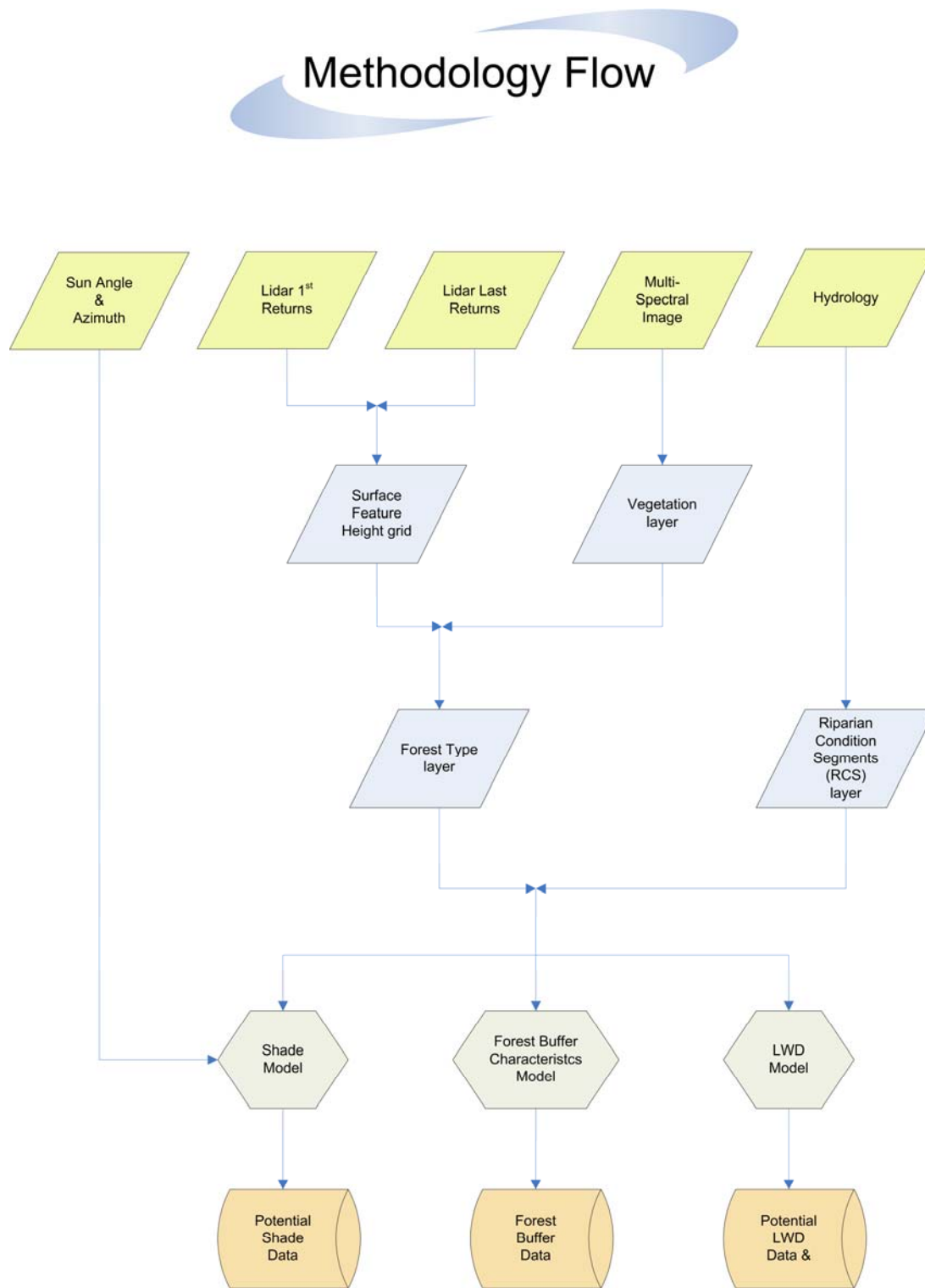


### 3.4 Model Overview

I designed this model with the goal of providing an objective method to remotely assess riparian area conditions using a system comprised of three primary sub-models developed using Visual Basic for Applications programs running within ESRI Inc.'s GIS software, ArcGIS (v. 9.1). Since the literature indicates that LWD recruitment and shade are primary factors in providing suitable salmon habitat, the LWD and Shade potential sub-models are primary components while the results of the Forest Buffer Characteristics sub-

model is considered secondary. Figure 3.8 below shows the overall methodology workflow developed for this study.

Figure 3.8 Methodology flow diagram.

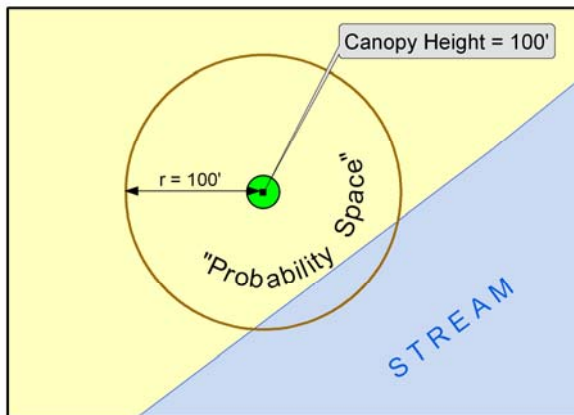


### 3.5 LWD model component

This sub-model component is based upon recognition of the fact that even in the most favorable circumstances, only a subset of the trees within a given forest may contribute LWD to a stream. LWD recruitment is a binomial phenomenon, meaning if some biological or physical event causes a tree to fall, the result is one of two simple possibilities: either it reaches the water or it does not (Cross, 2002). Additionally, the probability that any given tree within a riparian area will contribute LWD is a function of the tree's height and its distance from the edge of the stream (Robison and Beschta, 1990). It should be noted that the potential of a tree to contribute LWD to a stream is clearly different from the effectiveness of that LWD piece to create or improve the aquatic habitat within the stream via the formation of pools. Research has shown that the ability of the riparian forest to contribute adequate functional LWD to the adjacent stream is a function of the relationship between a given tree's diameter and the width of the adjacent watercourse (Beechie 1998, Beechie et al. 2000, Bilby and Ward 1989). The primary function of this LWD model is to quantify the potential LWD contribution from a given stretch of riparian forest to its adjacent watercourse. The model does not evaluate the effectiveness of the LWD pieces that may be contributed in terms of their diameter or relationship to the width of the watercourse.

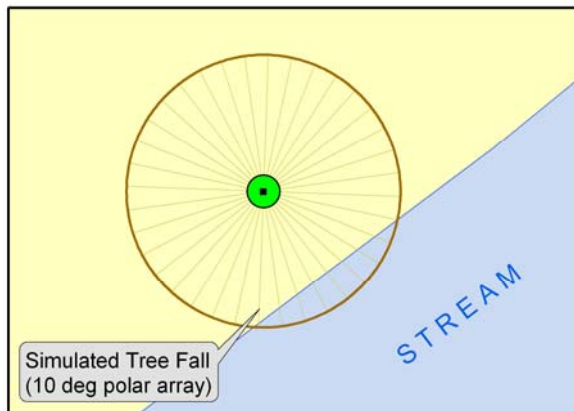
Cross (2002) defined the probability space of a given tree fall as a circle whose center is at the tree location having a radius equal to the height of the tree (Figure 3.9). When the tree falls, it must come down somewhere within that circle.

Figure 3.9 Probability space of a given tree fall whose radius is equal to tree height.



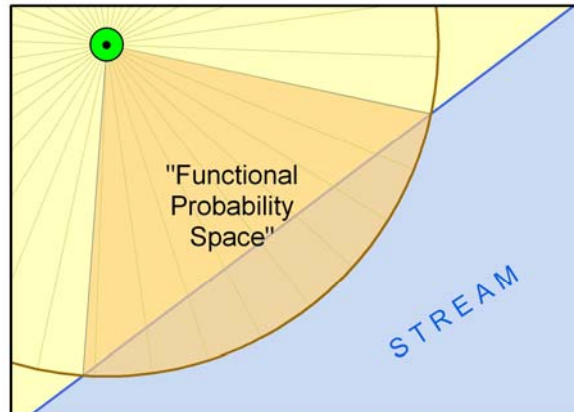
This model was based upon the assumption that the probability of a tree falling in any one direction is equal throughout the probability circle. Thus, neither ground slope nor prevailing wind direction are currently accounted for by the model. I designed this model to build upon Cross' LWD work by employing the concepts he developed regarding LWD and shade into a GIS model that can be applied to other study areas. The search for potential LWD recruited to the stream can be narrowed further by overlaying the probability space circle with the stream edge. For this study, I simulated tree fall by overlaying a polar array made up of lines placed at 10-degree intervals whose center is the tree location (Figure 3.10).

Figure 3.10 Simulated tree fall using a 10-degree polar array of lines equal to tree height.



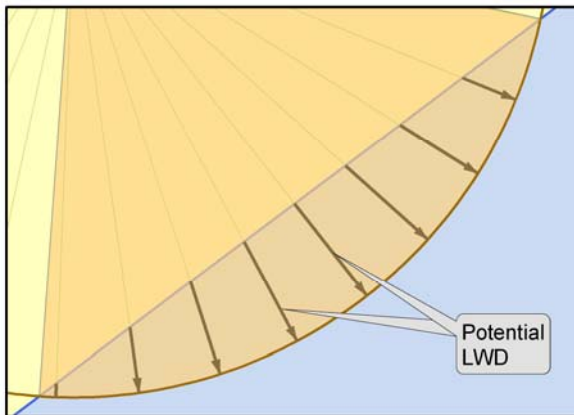
When an array and its probability space are overlaid with the stream edge, the probability space is reduced to the area common to both the tree height radius circle and the stream. I defined this area of intersection as the “Functional Probability Space” (Figure 3.11).

Figure 3.11 Functional probability space defined as the area common to both the tree height radius circle and the stream edge.



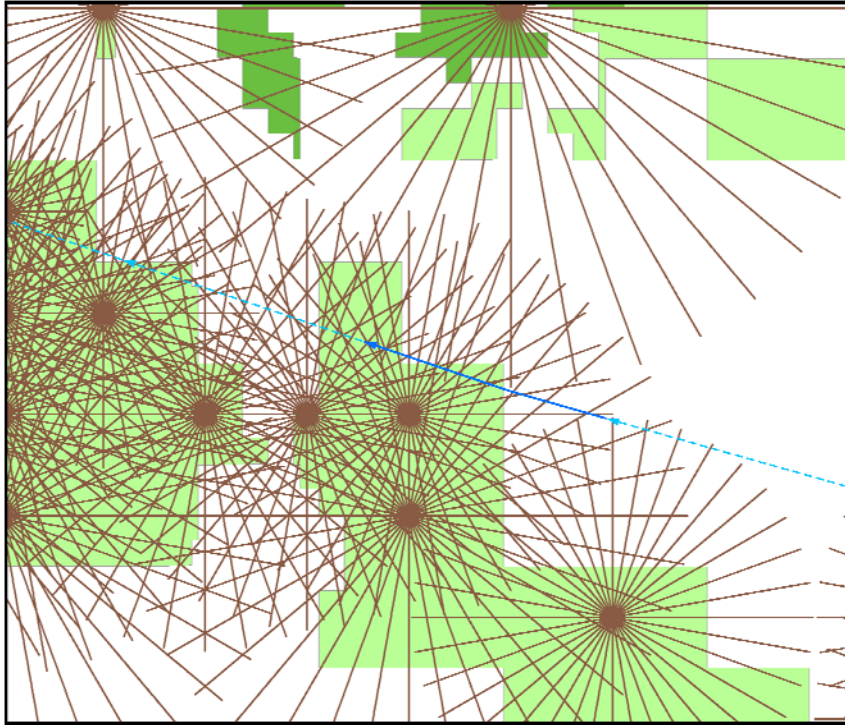
Finally, only those portions of the arrayed lines located within the functional probability space and intersecting the stream’s edge are identified as potential LWD pieces (Figure 3.12).

Figure 3.12 Potential LWD pieces.



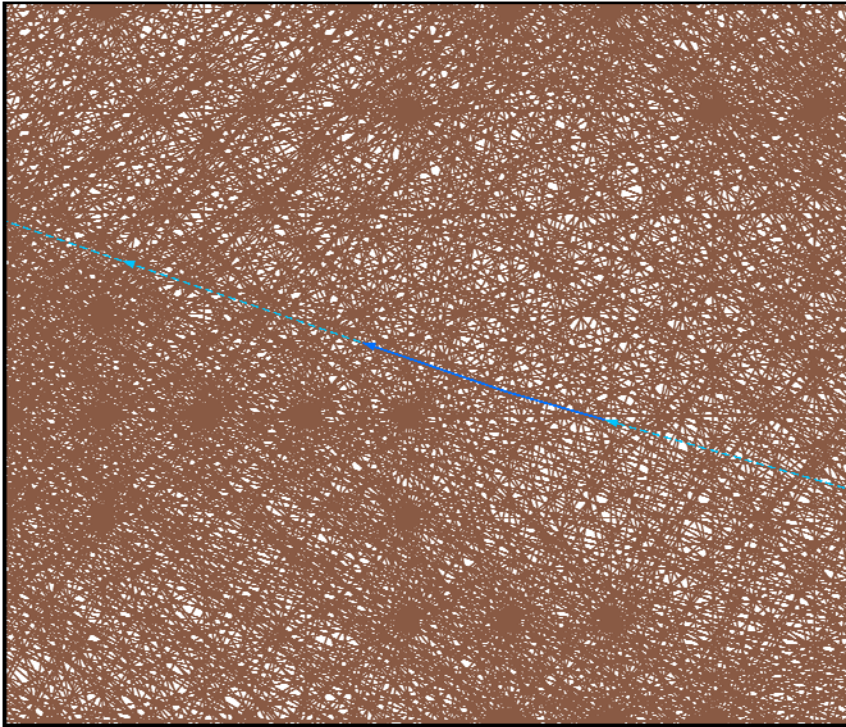
During a single run of the model, this process of creating potential LWD pieces using polar arrays to represent tree fall is performed twice on each candidate tree within the study area. For this model, I defined a candidate tree as a point located at the center of each 4-meter grid cell of the surface feature height grid whose height value is greater than 3 meters, whose probability circle intersects a watercourse edge, and whose location is within a conifer-dominant or deciduous-dominant polygon in the forest type layer. First, potential LWD pieces are created from arrays that consist of line lengths equal to height values generated from the lidar data in the surface feature height grid (Figure 3.13).

Figure 3.13 Study area example showing candidate tree fall arrays as brown lines created using lengths equal to lidar-generated height values. Dark green patches are conifer-dominant forest, while light green patches are deciduous-dominant forest.



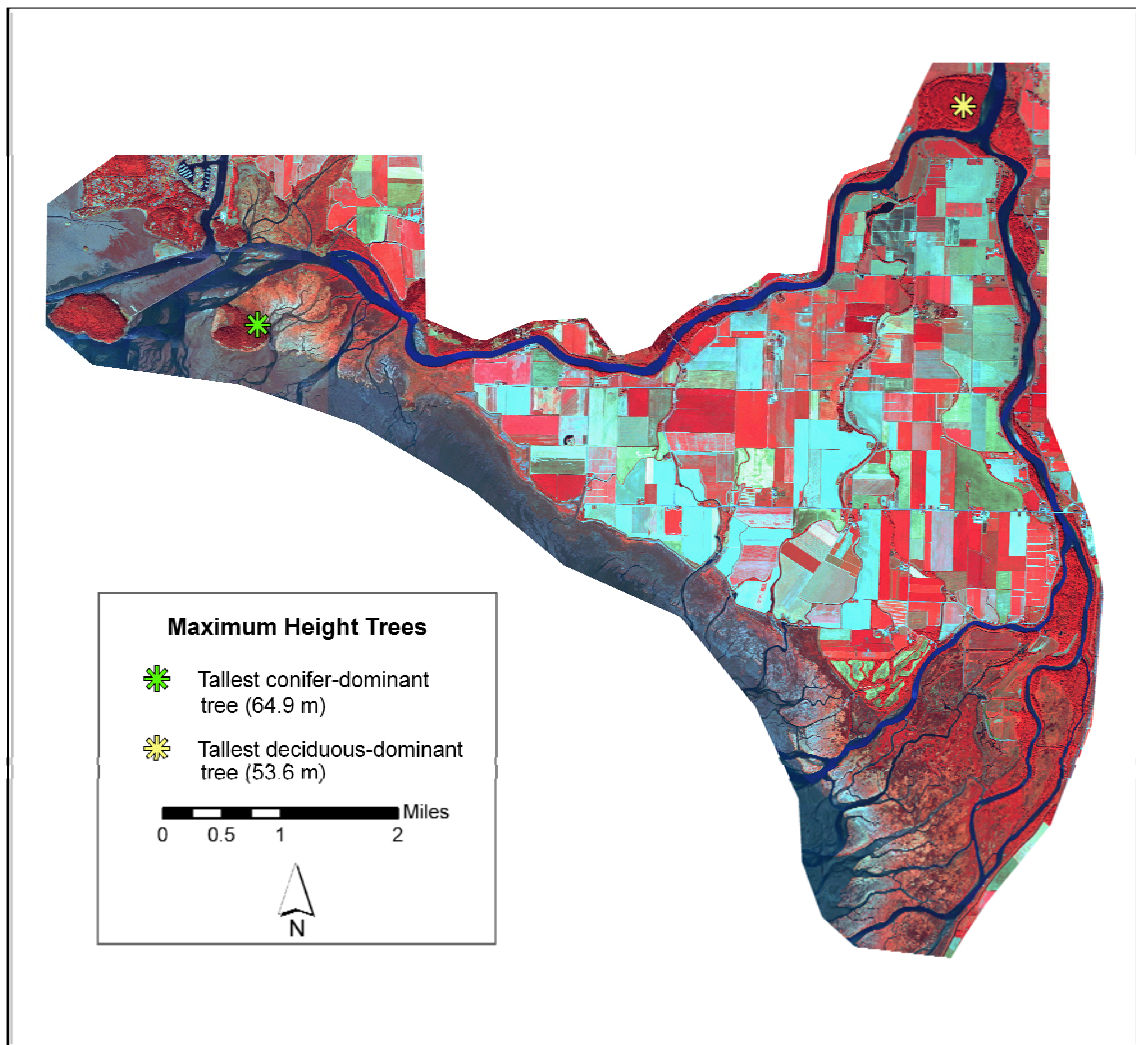
Next, a second set of potential LWD pieces are generated from new probability circles and polar arrays consisting of line lengths equal to the Maximum Study Area Height Tree (MSAHT) (Figure 3.14).

Figure 3.14 A second set of potential LWD pieces are generated using maximum study area trees.



I designed the model to identify both the maximum conifer-dominant and deciduous-dominant height values from the surface feature height grid cell points overlaid with the forest type layer. For this study area, a conifer-dominant MSAHT value of 64.9 meters and a deciduous-dominant MSAHT value of 53.6 meters were used to generate the second round of polar arrays representing potential LWD created in a situation where all candidate trees were replaced with trees equal to the maximum tree height within the study area. The locations of each tallest tree type within the study are shown in Figure 3.15.

Figure 3.15 Infrared view of the study area where MSAHT values were identified using the forest type layer overlaid with the surface feature height grid to identify the tallest conifer-dominant (64.9m) and deciduous-dominant (53.6m) tree heights within the study area.



All potential LWD recruitment pieces intersecting an RCS are then collected and seven basic LWD summary statistics for each RCS are calculated as follows:

- 1) Frequency (total number) of intersecting potential LWD pieces
- 2) Frequency (total number) of intersecting MSAHT potential LWD pieces
- 3) Minimum potential LWD piece length
- 4) Maximum potential LWD piece length

- 5) Mean potential LWD piece length
- 6) Standard Deviation of potential LWD piece lengths
- 7) LWD Index, calculated as follows:

$$(\text{Frequency Potential LWD} / \text{Frequency MSAHT LWD}) * 100$$

The LWD Index value is calculated by dividing the total number of intersecting LWD pieces by the total number of maximum study area height tree (MSAHT) LWD pieces and then multiplied by 100. Once the model run was completed, the LWD index value was used to give each RCS an LWD ranking so they can later be combined with other riparian characteristics to identify potential preservation and restoration sites. It should be noted that the minimum piece length, maximum piece length, mean piece length and standard deviation of piece lengths are statistics the model produces but were not used in this study since the LWD index values alone were sufficient when combined with other model-produced information to identify potential preservation and restoration sites within this study area. However, future applications of this model in other study areas may prove them useful. In this way, LWD Index values can be used to acquire information about the quantity of the potential LWD pieces that may currently be contributed to the stream as compared to the quantity of LWD that might be contributed if the existing riparian forest was allowed to reach the maximum study area tree height.

It is important to note that this LWD model has not been designed to consider forest density and its impacts to the potential shade produced by a riparian area since it selects candidate tree points located at the center of the 4-meter grid cells of the surface feature height grid.

### 3.6 Shade Model Component

By providing shade to an adjacent watercourse, riparian vegetation controls the amount of direct solar radiation that reaches that watercourse. Therefore, when riparian vegetation is removed, the amount of direct solar radiation a watercourse receives is increased which can result in higher diurnal temperature fluctuations (Barton et al. 1985, Brown and Krygier 1970, Vannote et al. 1980).

Since the position of the sun in the sky is a function of latitude, time of year and time of day, the azimuth and the altitude of the sun can be calculated. When this information is combined with riparian forest height and hydrology data, the potential shade produced by riparian forest adjacent to a stream can be estimated using right triangle trigonometry.

This potential shade production model builds upon the work by Cross (2002). The potential shade estimation via sun position and tree height concept he described were employed within this model in a GIS setting and then applied to the research study area. The model uses trigonometry and known positions of the sun combined with forest height and stream position data to estimate the shade provided to the adjacent water body by the vegetation within a given RCS. A sun azimuth of 208 degrees and an altitude of 55.3 degrees were used as the sun position input values for the shade model. These values were acquired from the U.S. Naval Observatory website for the study area on the same date and approximate time the DAIS 2001 multi-spectral image was acquired. Some initial simplifying assumptions and limitations for the shade model construction were as follows: ground slope was assumed to be zero and forest density is uniform throughout the study area.

In order to use a GIS to estimate the potential shade produced by a given tree, two

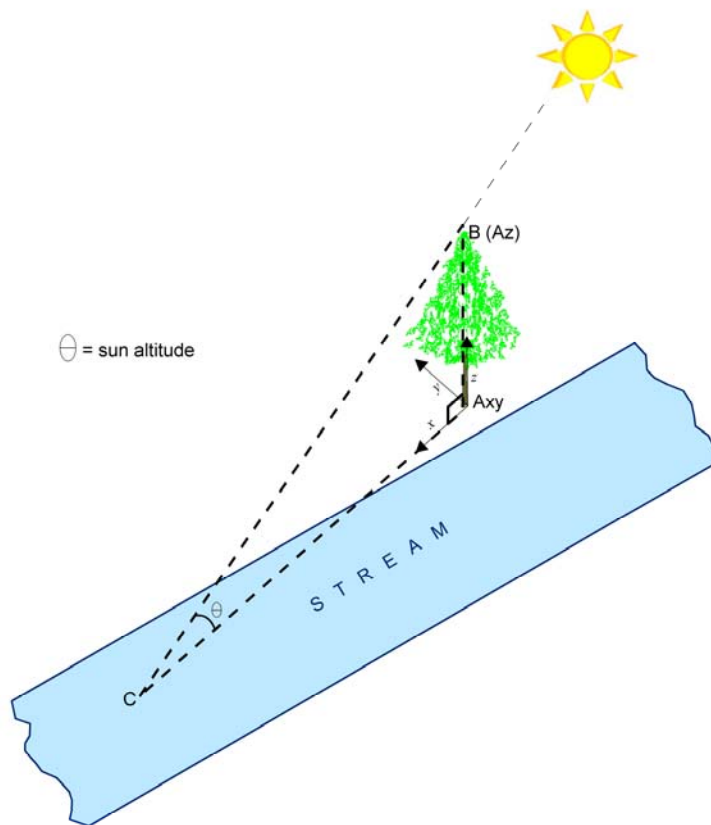
values must be determined:

- 1) The length of the shadow cast by the given tree.
- 2) The shadow direction, or location of the endpoint of the shadow cast by the top of the given tree.

Determining Shadow Length:

Let point A in Figure 3.16 represent a perspective view of a tree located at the center of a given cell in the surface feature height grid (and also located within a forested area of the forest type layer), having a known location of  $A_x, A_y$  on the ground and whose z-value represents the forest height at that point.

Figure 3.16 Sun position and tree height are used to estimate shadows.



The value of the cell at point A then is the height (Az) of the given tree located at point A. Therefore, the length of side AB of the right triangle ABC is known. AB is also known as the opposite length of the same right triangle. Let  $\theta$  be the sun altitude angle. Using the following trigonometric relationship to solve for the length of the adjacent side of the triangle ABC gives:

$$(1) \quad \tan\theta = \text{opposite side length} / \text{adjacent side length}$$

Solving for the adjacent side length, known as AC in Figure 3.16 gives:

$$(2) \quad \text{adj length} = \text{opp length} / \tan\theta$$

Thus, the value of side AC represents the length of the shadow cast by a given tree located at point A with a known sun altitude for a given date and time. Although side BC is the actual length of the shadow cast, side AC is the value used in this model since we are using typical 2-dimension (top-down view) raster and vector data.

Part 2) Determining Shadow Direction:

Let M in Figure 3.17 represent a top down view of a given tree located at M in the surface feature height grid and also within a forested area of the forest type layer. Let L be the known location of the sun, having an azimuth of 208 degrees East of North for August 7th, 2001.

Figure 3.17 Top-down view of a tree located at M and sun azimuth of 208 degrees.

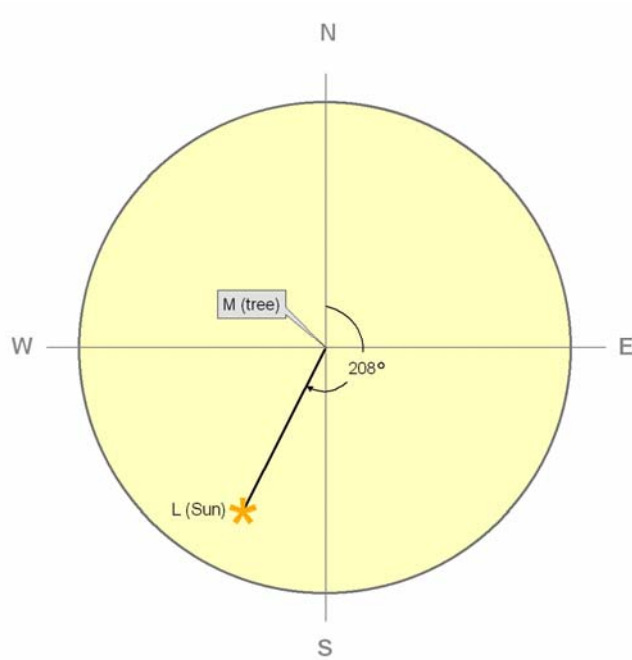
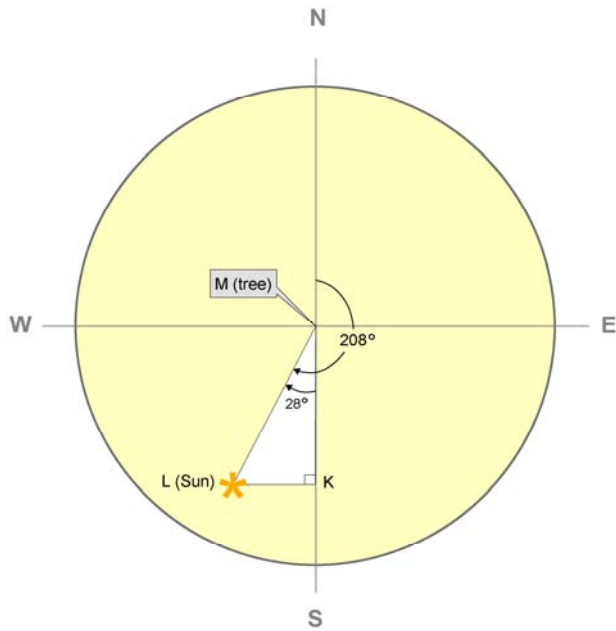


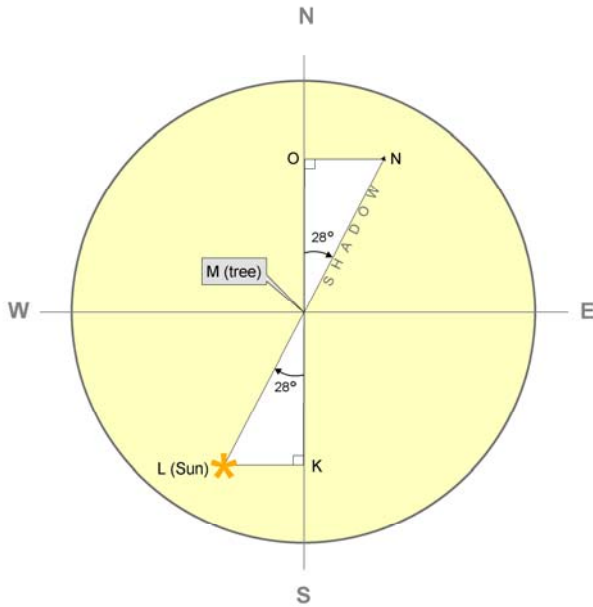
Figure 3.17 shows that with a sun azimuth angle of 208 degrees East of North on August 7th, 2001, the sun is located in the SW quadrant given by an angle turned 208 degrees east from North. This creates the right triangle KLM shown in Figure 3.18.

Figure 3.18 Right triangle KLM.



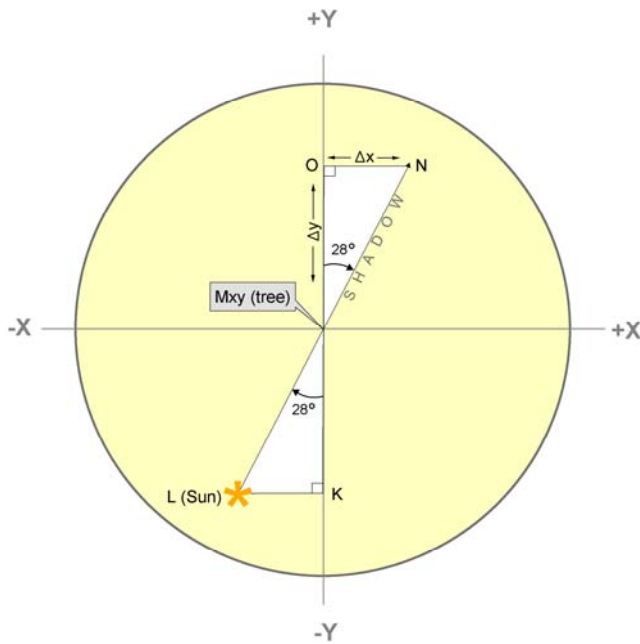
Using the trigonometric rule of complimentary angles, a shadow cast by a tree at point M will fall within the NE quadrant and form the right triangle MNO shown in Figure 3.19.

Figure 3.19 Side MN of right triangle MNO represents the shadow cast by a tree located at point M.



The hypotenuse side of the right triangle MNO, shown as length MN in Figure 3.19, represents the shadow cast by a tree located at point M. The length of this side was determined previously in part 1, Determining Shadow Length. Figure 3.20 replaces the North-South axis of the compass rose with the Y-axis of a Cartesian coordinate system. Similarly, the East-West axis is replaced by the X-axis of a Cartesian Coordinate system.

Figure 3.20 Length MO represents change in Y-direction and ON represents the change in X-direction for the shadow's endpoint.



The adjacent side, length MO, now represents the change in the Y-direction of the shadow cast by the tree at point M, while the opposite side, length ON, represents the change in X-direction of the same. The length of the adjacent side, MO, can be determined using the following trigonometric relationship:

$$(1) \cos(\sigma) = \text{adjacent side length} / \text{hypotenuse side length}$$

Solving the above equation for the adjacent side, MO, gives:

$$(2) \text{adj length (MO)} = \cos(\sigma) * \text{hyp length}$$

Similarly, the length of the opposite side, ON, can be determined using the following trigonometric relationship:

$$(3) \sin(\sigma) = \text{opposite side length} / \text{hypotenuse side length}$$

Solving the above equation for the opposite side, ON, gives:

$$(4) \text{ opp length (ON)} = \sin(\sigma) * \text{hyp length}$$

Since the change in the X direction ( $\Delta x$ ) represented by ON is in the positive direction shown in Figure 3.20, it is added to  $M_x$ . Since the change in Y direction ( $\Delta y$ ) represented by side MO is in the positive direction along the Y-axis (Figure 6), it is added to  $M_y$ . Thus, the following equation gives the x-coordinate location of the point N:

$$(5) N_x = M_x + ON$$

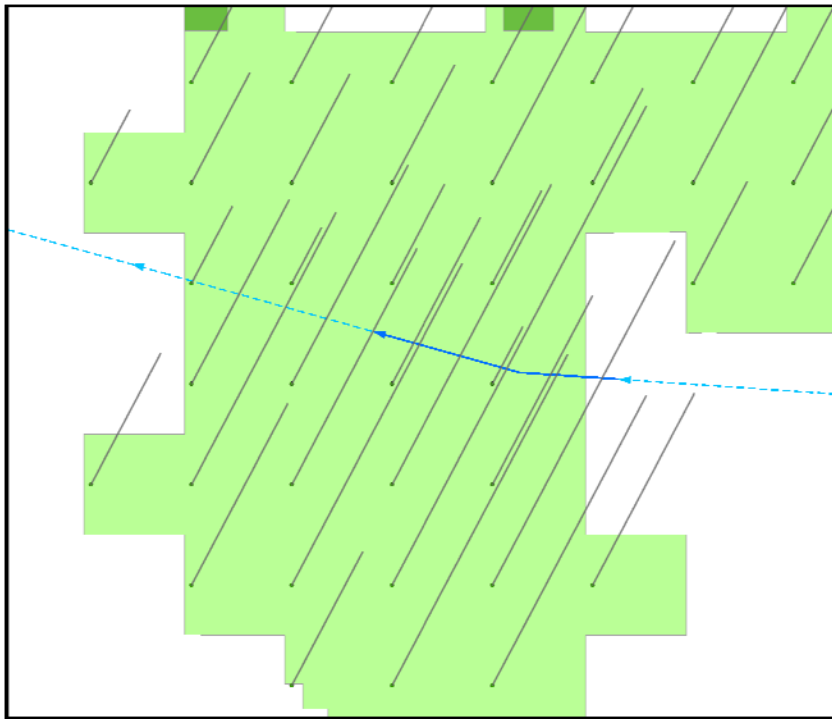
The following equation gives the y-coordinate of the point N:

$$(6) N_y = M_y + MO$$

Together,  $N_x N_y$  represent the location of the endpoint of the shadow cast by a tree at point M in the surface feature height grid. Using similar methodology as that employed in the LWD model, the shade production model performs these previous calculations for all

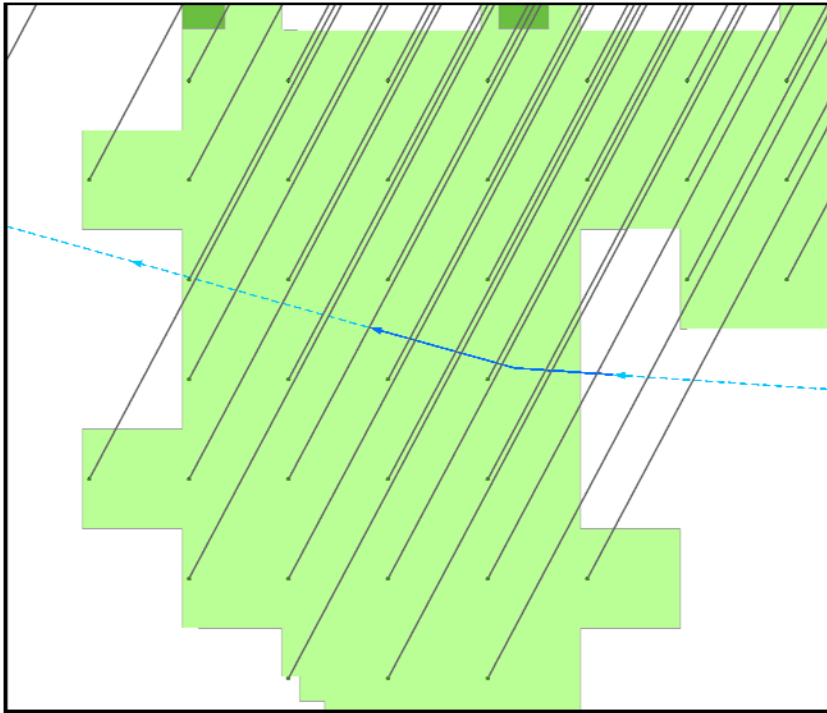
candidate trees twice. For this model component, I defined a candidate tree as a point located at the center of each grid cell of the surface feature height grid whose height value is greater than 3 meters, whose generated shadow is of sufficient length to intersect the adjacent watercourse edge, and whose location is within a conifer-dominant or deciduous-dominant polygon in the forest type layer. First, potential shadows are created for candidate trees using height values generated from the lidar data in the surface feature height grid (Figure 3.21).

Figure 3.21 Study area example of candidate tree shadows generated using lidar-generated tree height values.



Next, a second set of potential shadows are generated from new tree height values equal to the same maximum study area height trees (MSAHT) identified earlier for both conifer-dominant and deciduous dominant forest (Figure 3.22).

Figure 3.22 Potential shadows generated using MSAHT values.



All shadows intersecting each RCS are collected and summary statistics, similar to those created for potential LWD pieces, are generated.

- 1) Frequency (total number) of intersecting shadow lines
- 2) Frequency (total number) of intersecting maximum site tree potential (MSAHT) shadow lines
- 3) Minimum potential shadow length
- 4) Maximum potential shadow length
- 5) Mean potential shadow length
- 6) Standard Deviation of potential shadow lengths

7) Shade Index, calculated as follows:

$$(\text{Frequency Potential Shadows} / \text{Frequency MSAHT Shadows}) * 100$$

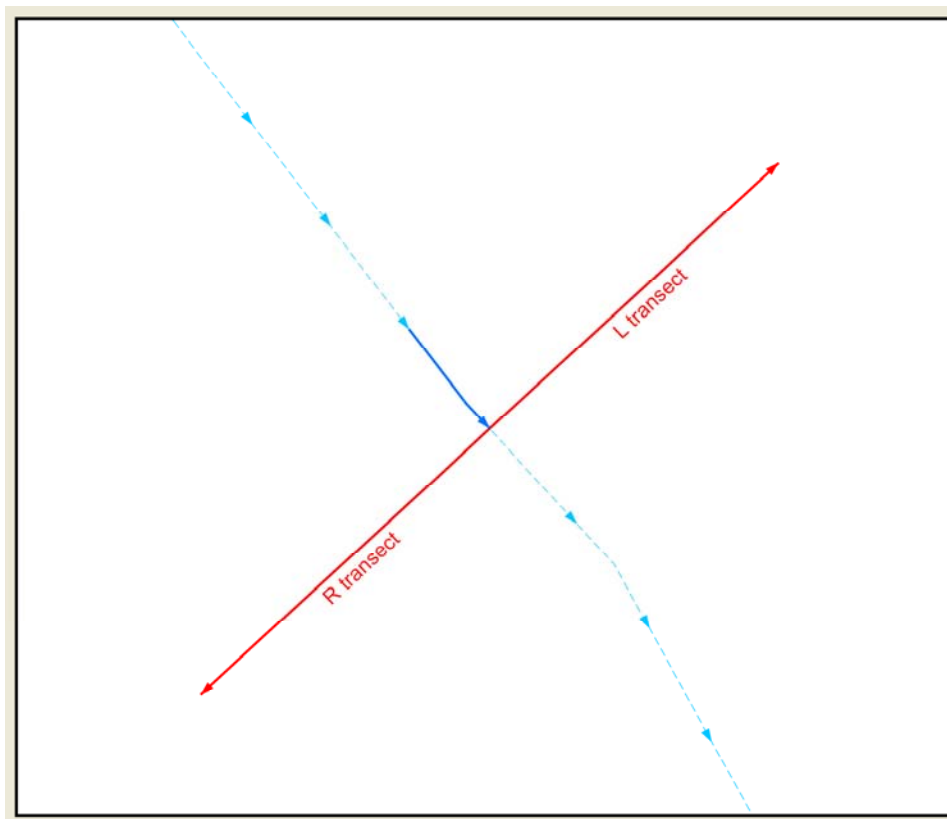
The Shade Index value is calculated by dividing the total number of intersecting shadow lines by the total number of maximum study area height tree (MSAHT) shadow lines and then multiplied by 100. Once the model run was completed, the values above were used to give each RCS a shade ranking so they can later be combined with the LWD rankings and other riparian characteristics to identify potential preservation and restoration sites. It should be noted that the minimum shadow length, maximum shadow length, mean shadow length and standard deviation of shadow line lengths are statistics the model produces but were not used in this study since the shade index values alone were sufficient when combined with other model-produced information to identify potential preservation and restoration sites within this study area. However, future applications of this model in other study areas may prove them useful. Using this methodology, shade index values can be used to acquire information regarding the quantity of the shade that may currently be contributed to the stream as compared to the quantity of shade that might be contributed if the existing riparian forest was allowed to reach the maximum study area tree height.

It is important to recognize that this shade model has not been designed to consider forest density and its impacts to the potential shade produced by a riparian area since it locates candidate tree points at the center of the 4-meter grid cells of the surface feature height grid.

### 3.7 Forest Buffer Characteristics Model Component

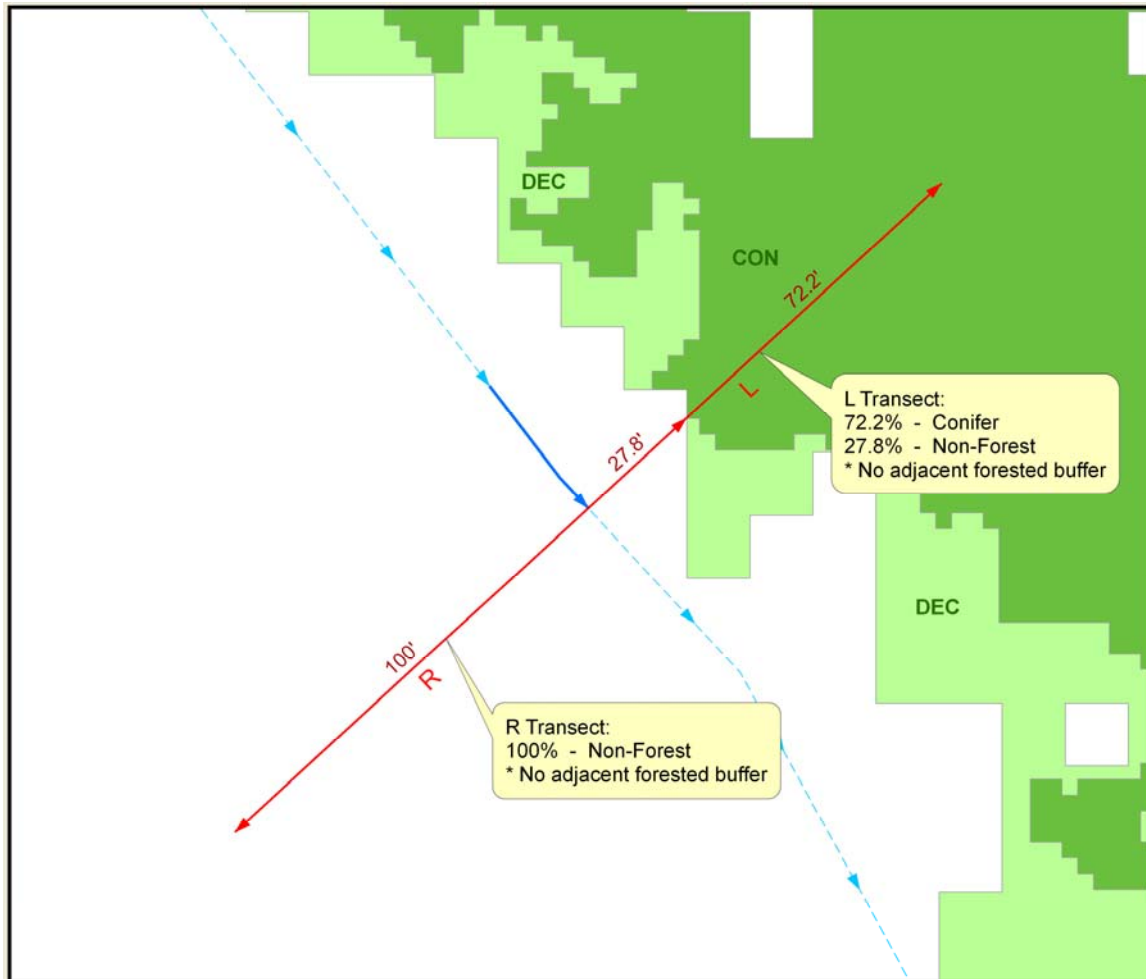
This model allows the user to enter a buffer distance, which is essentially the distance into the riparian area moving away from the watercourse that will be used to assess the riparian area's characteristics. For the current application, I used a buffer distance of meters (approximately 100'). A transect pair, each side measuring 30 meters (approximately 100') in length was inserted at the endpoint of and perpendicular to each RCS (Figure 3.23).

Figure 3.23 Right and left 30-meter length transects are placed at the endpoint of each RCS.



At this point, the forest type layer is intersected with the transect pair, thus subdividing the transects into smaller pieces (Figure 3.24).

Figure 3.24 Transects are subdivided into smaller pieces by overlaying the forest type layer.



These pieces are then tallied, summarized and recorded for each RCS according to their forest type and lengths to create the following secondary riparian zone characteristics that can later be combined with the primary riparian zone characteristics, LWD and shade, to help identify potential preservation and restoration sites within the study area:

- Right and left adjacent forest buffer width
- Right and left adjacent forest type
- Right and left % Deciduous-dominated

- Right and left % Conifer-dominated
- Right and left % No forest canopy

These characteristics are used later when combined with the primary riparian zone characteristics, LWD and shade, to help filter out potential preservation and restoration sites within the study area.

## 4.0 Results and Discussion

### *4.1 Forest Type Accuracy Assessment*

The forest type layer used in this research was created using remote sensing feature extraction software. Three categories were classified from the DAIS color imagery into a GIS data layer consisting of conifer-dominant polygons, deciduous-dominant polygons, and non-forested polygons. Within the study area, 35 sites were visited in order to assess the forest type layer for accuracy. The field-assessed sites adequately matched the forest type layer with an overall classification accuracy of 91%. Due to right of entry issues on private property and difficult field accessibility for many locations within the study area, only 35 sites were visited. Originally, all sites were selected at random, however due to the aforementioned right of entry issues on private property and field logistics, sampling site locations were adjusted accordingly. Sites were assessed qualitatively and recorded as one of the three forest type data layer classifications: conifer-dominant, deciduous-dominant and non-forested. The recorded field data are compared with the forest type data layer and an error matrix (Congalton et al. 2002) was used to develop an accuracy assessment (Table 4.1).

Table 4.1 Forest type layer accuracy assessment error matrix from 35 field visited sites.

		DEC	CON	NON	row total	Users Accuracy	
Forest Type Layer	DEC	22	1	1	24	92%	
	CON	1	5	0	6	83%	
	NON	0	0	4	4	100%	
	col total	23	6	5	34		
Producers Accuracy		96%	83%	80%		91%	Overall Accuracy

Error matrix calculations showed an overall classification accuracy of 91% (Table 4.1). The producer's accuracy ranged from 83% to 96% while the users accuracy was between 92% and 100%.

#### 4.2 Model Results Accuracy Assessment

In order to verify the accuracy of the LWD and shade model components, LWD index and shade index values were manually calculated for 36 randomly selected RCSs within the study area. The manually calculated LWD index matched the model calculated value for 35 of the 36 sites or 97.2% of the time. The single incorrect value was within 1% of the value calculated by the model and appeared to be due to a rounding error. The manually calculated shade index values matched the shade index values calculated by the shade model for 34 of 36 sites or 94.4% of the time. Again the two incorrect values appeared to be due to rounding errors.

In order to verify the accuracy of the forest buffer characteristics model, the adjacent forest buffer width and the percent of the buffer consisting of conifer-dominant forest were evaluated via photo interpretation using the DAIS multi-spectral imagery. For adjacent forest buffer width, the photo interpreted values correctly matched the model-calculated values for 32 of the 36 sites or 88.8% of the time. The difference between the photo-interpreted values and those calculated by the model appeared to be primarily due to my inability to detect the difference between lower vegetation such as shrubs from forested vegetation during photo interpretation since the multi-spectral imagery alone does not provide any information about the height of the vegetation.

The percent of the buffer consisting of conifer-dominant forest was also evaluated via photo interpretation. The photo-interpreted percent conifer values matched the values calculated by the forest buffer characteristics model for 33 of the 36 sites or 91.7% of the time. The difference between the model-calculated and photo interpreted values here appeared to be due to the difficulties in accurately assessing a percentage of conifer-dominant forest along the transect pairs by eye.

#### 4.3 LWD Potential

An LWD ranking of 1 through 10 was assigned to each RCS based on its LWD index value (Table 4.2). An RCS with an LWD index greater than or equal to 0 and less than 10 resulted in an LWD ranking of 1. Likewise, an LWD index value greater than or equal to 90 received an LWD ranking of 10. The larger the LWD rank assigned a given RCS, the more likely its adjacent riparian area has the potential to provide it with a maximum study area height tree, thus making it a better candidate for preservation efforts.

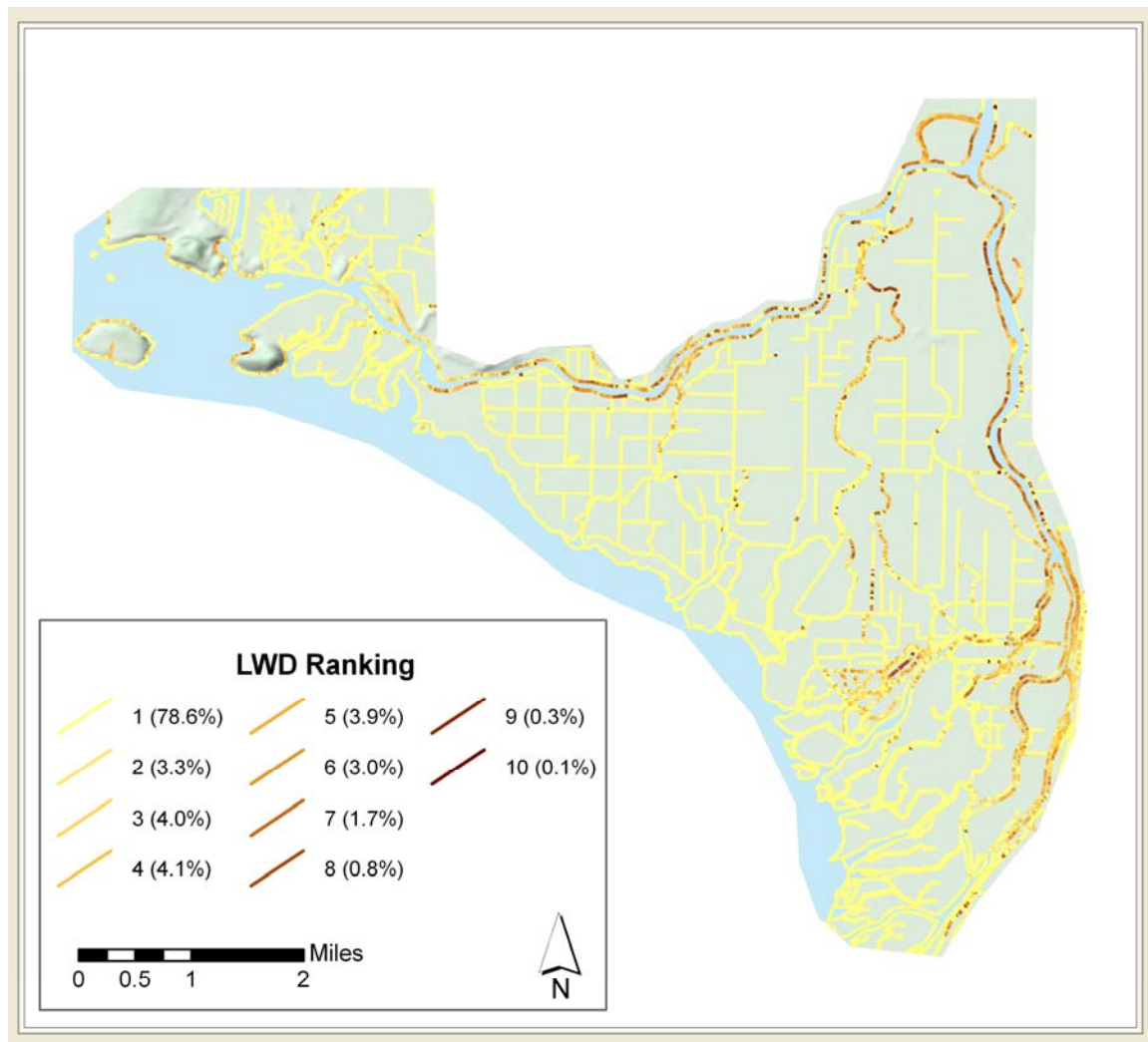
Likewise the lower the LWD ranking, the more likely a riparian area does not have the potential to contribute LWD to its adjacent RCS, thus indicating the given RCS may be a good candidate for restoration activities.

Table 4.2 LWD rankings 1-10 assigned according to LWD Index values.

<b>LWD Index</b>	<b>Total RCSs</b>	<b>% Total</b>	<b>Rank</b>
0 – 10	31715	78.6%	1
10 – 20	1343	3.3%	2
20 – 30	1630	4.0%	3
30 – 40	1654	4.1%	4
40 – 50	1584	3.9%	5
50 – 60	1219	3.0%	6
60 – 70	687	1.7%	7
70 – 80	327	0.8%	8
80 – 90	122	0.3%	9
90 – 100	60	0.1%	10

Nearly 80% of the total RCSs within the study area resulted in an LWD Index of less than 10, therefore receiving a rank of 1 (Table 4.2). Only 0.1% of the total RCSs within the study area resulted in an LWD rank of 10. These results are not surprising given that the study area’s land use is primarily agricultural and much of the riparian forest has already been removed. Most of the high LWD ranking occurred along the larger water features along the eastern and northwestern portions of the study area (Figure 4.1).

Figure 4.1 Map showing LWD ranking of RCSs where lower values indicate decreased potential LWD contribution and larger values indicate increased potential LWD contribution.



It is important to emphasize that this model does not account for ground slope adjacent to the stream or within the streambed itself nor does it test for the effectiveness of the potential LWD pieces that can be contributed to an adjacent waterway.

#### 4.4 Shade Potential

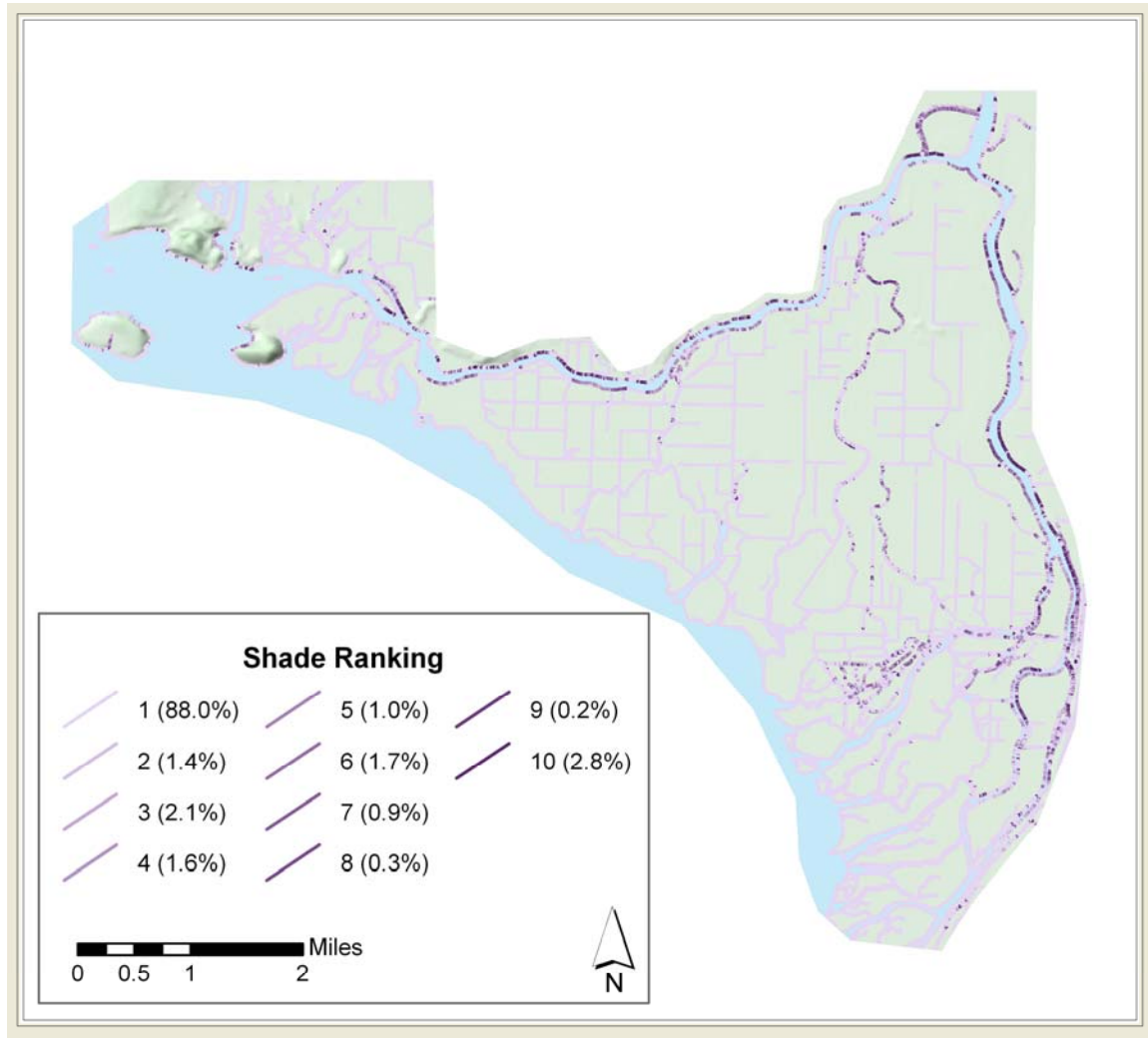
A potential shade ranking was assigned to each RCS based on its Shade Index value (Table 4.3). At least 88% of the RCSs within the study area showed a shade index of less than 10 while only 2.8% of the study area RCSs resulted in a shade index of 10. As with LWD rankings, the larger the shade rank the more likely a riparian area has the potential to provide a maximum shade to its adjacent watercourse RCS, therefore making it a better candidate for preservation efforts. Likewise, the lower the shade rank, the more likely a riparian area does not have trees of sufficient height to provide maximum shade, indicating these RCSs may be good candidates for restoration activities.

Table 4.3 Shade rankings 1-10 assigned according to Shade index values.

<b>Shade Index</b>	<b>Total RCSs</b>	<b>% Total</b>	<b>Rank</b>
0 – 10	35524	88.0%	1
10 – 20	705	1.4%	2
20 – 30	719	2.1%	3
30 – 40	759	1.6%	4
40 – 50	789	1.0%	5
50 – 60	238	1.7%	6
60 – 70	280	0.9%	7
70 – 80	174	0.3%	8
80 – 90	42	0.2%	9
90 – 100	1111	2.8%	10

As with the LWD index, the RCSs with the highest shade index values occurred along the eastern and northwestern portions of the study area (Figure 4.2).

Figure 4.2 Map showing RCS shade rankings where lower values indicate decreased shade potential and larger values indicate increased shade potential.



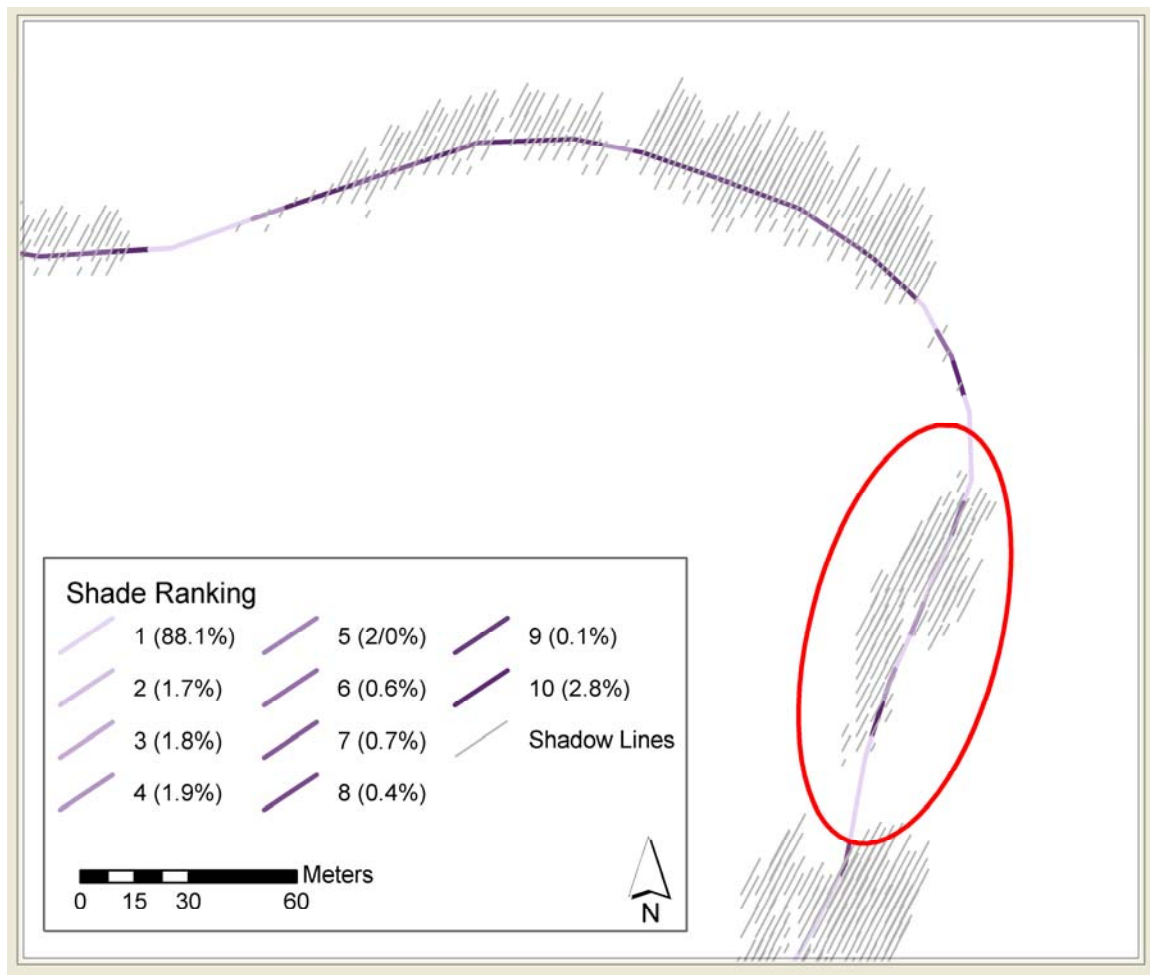
It is important to note that the shade model does not consider forest density since this model places a candidate tree at the center of each 4-meter cell of the surface feature height grid and also located within a forested patch of the forest type layer.

The shade sub-model was designed to estimate shadow lines for a specific date and time, where the sun is specifically positioned in the sky accordingly. Therefore, there is some bias towards those watercourses primarily oriented in an east-west direction in regards

to shading due to the position of the sun and thus the angle of the shadow lines generated.

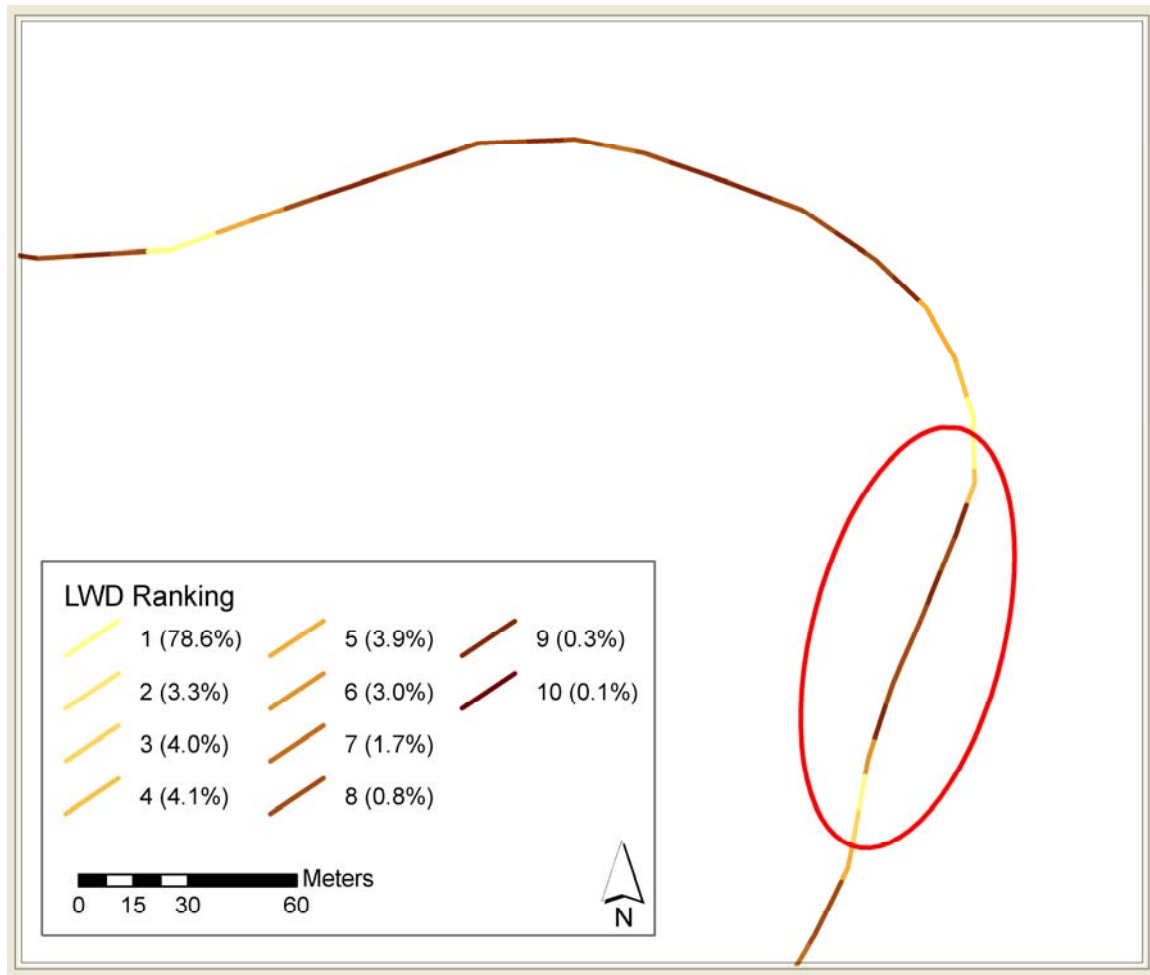
Figure 4.3 shows an example of this bias where the potential shadow lines the model is designed to generate are angled due to sun position so that they fail to intersect many of the north-south stretches of watercourse. As a result, it is likely the shade ranking applied is under-estimated.

Figure 4.3 Shading bias is observed here for the portion of this stream oriented in an east-west direction over the portion of the stream having a more north-south orientation (circled in red).



In these cases, the LWD Index is unaffected because the potential LWD arrays cover a 360-degree circle. Figure 4.4 shows this same portion of north-south oriented stream and its LWD ranking.

Figure 4.4 LWD Index is not affected by the bias as Shade Index due to potential LWD polar arrays that cover 360-degrees.

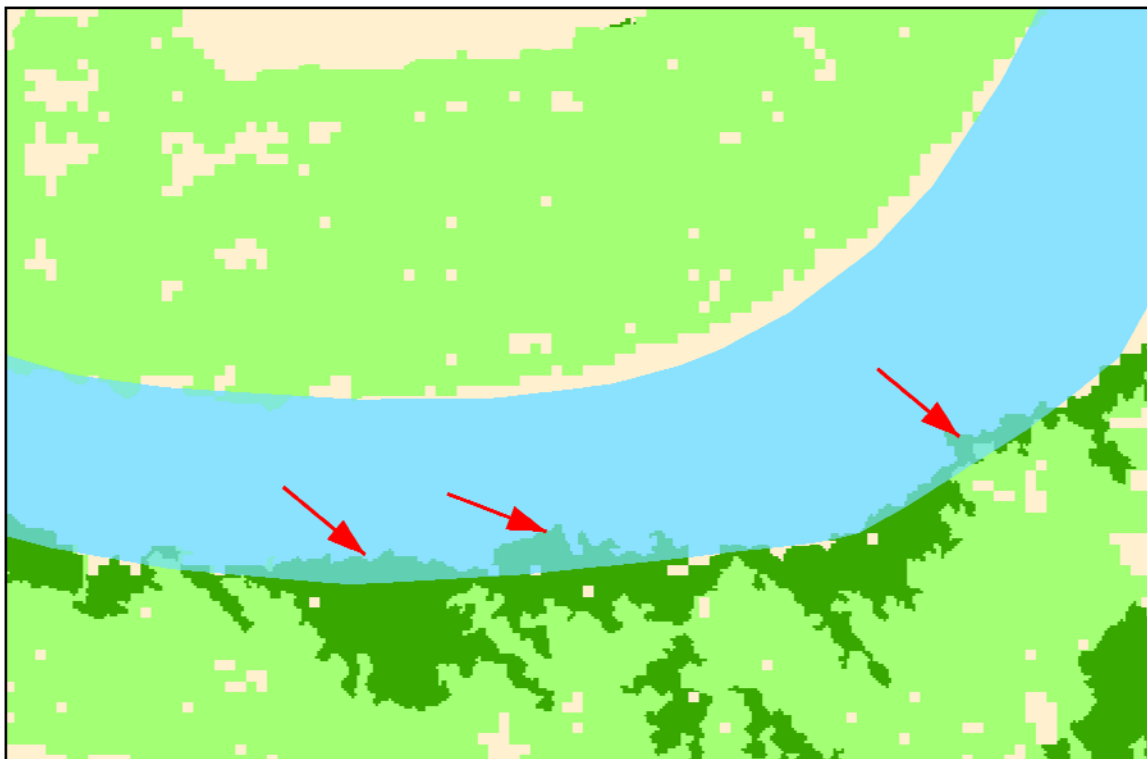


Additionally, an east-west stretch of watercourse where no trees currently exist on its south side, but contains trees on its north side would likely not rank well for shade since its

possible that no shadow lines would be created that intersect the south bank of the watercourse.

While this model is primarily intending to evaluate the riparian area adjacent to a waterway, it can also be used to determine how much of a waterway is covered by overhanging vegetation within the study area (Figure 4.5). I intersected the forest type layer with the hydrology layer's water bodies and only 1.4% of the water bodies in the study area were shaded by overhanging forest canopy vegetation.

Figure 4.5 Overhanging coniferous and deciduous forest canopy vegetation.



#### 4.5 Secondary Riparian Area Characteristics

The secondary riparian characteristics the model was designed to analyze are forest buffer width and forest buffer type. It is important to note that the model was designed to measure the width of the continuous adjacent buffer only and therefore the user is required to enter an “Adjacency Tolerance” value prior to analyzing any secondary riparian area characteristics. For this study, I input a tolerance of 5 feet to the model which effectively defined “adjacent forest” for this model run as forest located within 5 feet of an RCS. Upon model completion, a forest buffer width ranking was assigned to each RCS based on the percent of existing adjacent forested buffer on at least 1 side of the segment (Table 4.4).

Table 4.4 Forest buffer width rankings 1-10 assigned according to the percentage of the buffer that is forested located adjacent to the RCS.

<b>Forest Buffer Width</b>	<b>Total RCSs</b>	<b>% Total</b>	<b>Rank</b>
0 - 10%	35070	86.9%	1
10 - 20%	696	1.7%	2
20 - 30%	563	1.4%	3
30 - 40%	452	1.1%	4
40 - 50%	415	1.0%	5
50 - 60%	296	0.7%	6
60 - 70%	344	0.9%	7
70 - 80%	218	0.5%	8
80 - 90%	224	0.6%	9
90 - 100%	2063	5.1%	10

\*Rankings were assigned even if only 1 side of an RCS meets the "Forest Buffer Width" criteria listed.

For this study, I assigned rankings based on the adjacent forest buffer width present on one side of an RCS. This means, for example, that in order for an RCS to receive a ranking of 5, it was required to have 40-50% of its buffer forested on only one side. Likewise, an RCS having 40-50% on both sides would also receive a ranking of 5. In addition to forest buffer width data, information was also obtained regarding the amount of each forest type present

along the transect pairs of each RCS. As with forest buffer width, this information was used to apply a similar ranking system (Table 4.5) where only one side of the RCS was required to meet a given percentage in order to receive the appropriate rank value. Approximately 86.9% of the study area RCSs, indicated less than 10% of the buffer consists of conifer-dominant forest, while only 5.1% resulted in a buffer consisting of more than 90% conifer-dominant forest.

Table 4.5 Percent buffer conifer-dominant rankings 1-10 assigned according to the percentage of the buffer that consists of conifer-dominant forest. The forest may or may not be adjacent to the RCS.

<b>% Buffer Conifer-Dominant</b>	<b>Total RCSs</b>	<b>% Total</b>	<b>Rank</b>
0 - 10%	38188	94.7%	1
10 - 20%	497	1.2%	2
20 - 30%	378	0.9%	3
30 - 40%	279	0.7%	4
40 - 50%	230	0.6%	5
50 - 60%	179	0.4%	6
60 - 70%	179	0.4%	7
70 - 80%	166	0.4%	8
80 - 90%	122	0.3%	9
90 - 100%	123	0.3%	10

\*Rankings are assigned even if only 1 side of an RCS meets the "% Buffer Conifer-Dominant" criteria listed.

Only 7.8% of the RCSs resulted in at least one side of their adjacent riparian buffers consisting of 50% forested cover. Of those, only 0.5% also resulted in a minimum of 50% of their adjacent forested buffer consisting of conifer-dominant forest. Those with at least 50% of the buffer consisting of deciduous-dominant forest made up 7.1% of the total RCSs.

#### 4.6 Ranking Riparian Conditions

One key aspect of this model is that it allows the user to determine his/her own way of organizing and ranking the RCSs. Since the model can be used to generate a variety of

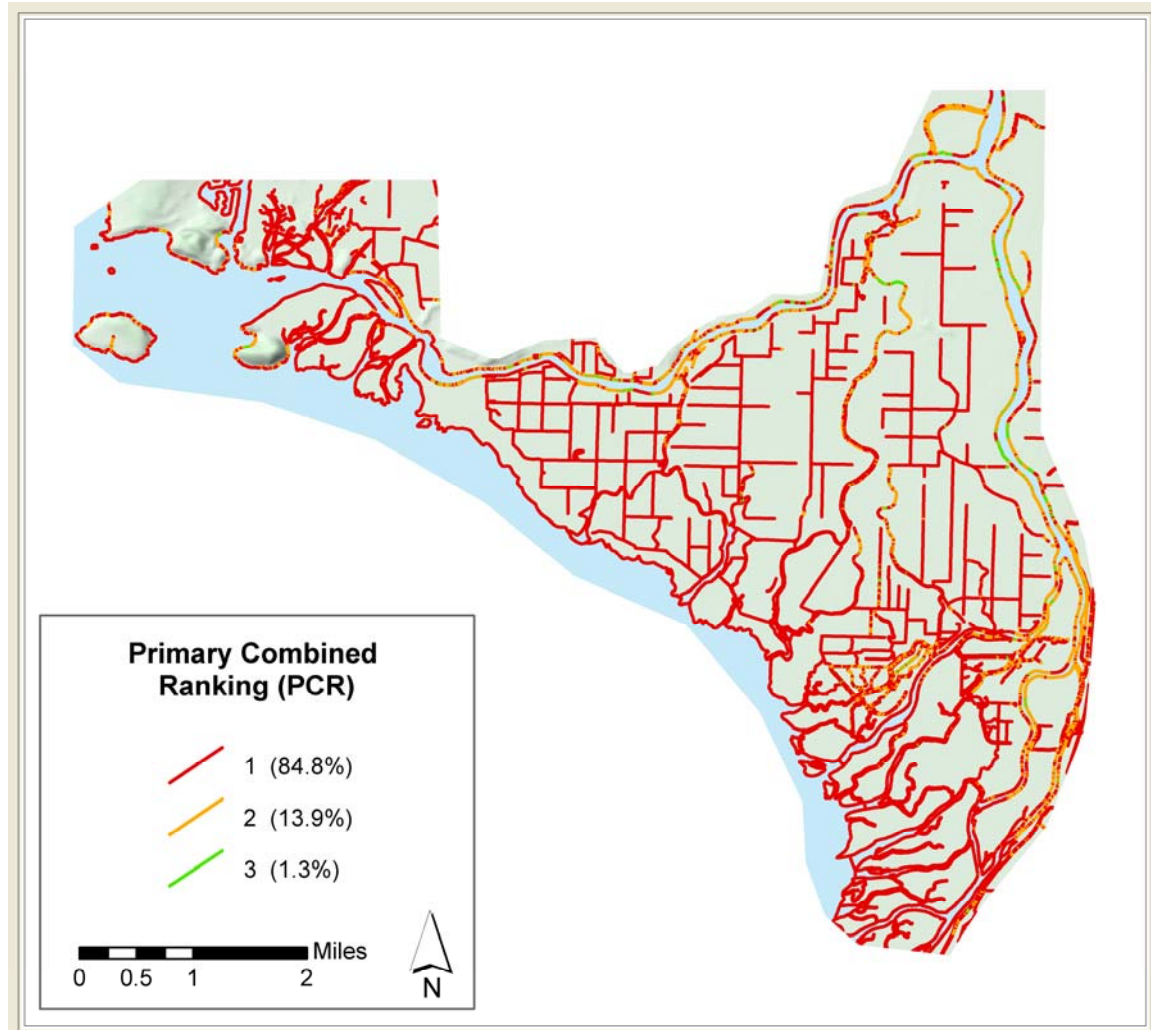
indices and summary statistics, the user can use this information to rank sites based on different aspects of riparian structure and function. To provide an integrated assessment of riparian conditions for this research, the LWD model results were combined with shade and forest buffer width results to identify sites (RCSs) having the highest priority for restoration or preservation activities. Since the purpose of this research was to develop a model primarily focused on LWD recruitment and shade production, the first step in creating a combined ranking was to apply a simple three-level ranking to each RCS by merging the two primary function indices, LWD index and shade index values. Table 4.6 shows how the LWD and shade indices were combined to formulate the primary combined ranking (PCR).

Table 4.6 LWD index and shade index were combined to create a primary combined rank (PCR) value for each RCS.

<b>Primary Combined Rank (PCR)</b>	<b>Total RCSs</b>	<b>% Total</b>	<b>Rank</b>
LWD & Shade Index <= 3	34224	84.8%	1
LWD & Shade Index >= 4 AND <= 6	5606	13.9%	2
LWD & Shade Index >= 7	511	1.3%	3

The PCR values were established as follows: All RCSs with an LWD Rank between 1-3 and a Shade Rank between 1-3 received a PCR value of 1 or “poor”. All RCSs having and LWD Rank between 7–10 and a Shade Rank value of 7-10 received a PCR value of 3 or “good”. All remaining RCSs received a PCR value of 2 or “moderate”. Only 1.3% received PCR values of 3 or “good”, while 84.8% of the total study area resulted in a PCR value of 1 or “poor.” A total of 13.9% of the study area received a PCR value of 2 or “moderate.” Finally, a map was generated showing the PCR values for the entire study area (Figure 4.6).

Figure 4.6 Map of PCR values for each RCS within the study area.

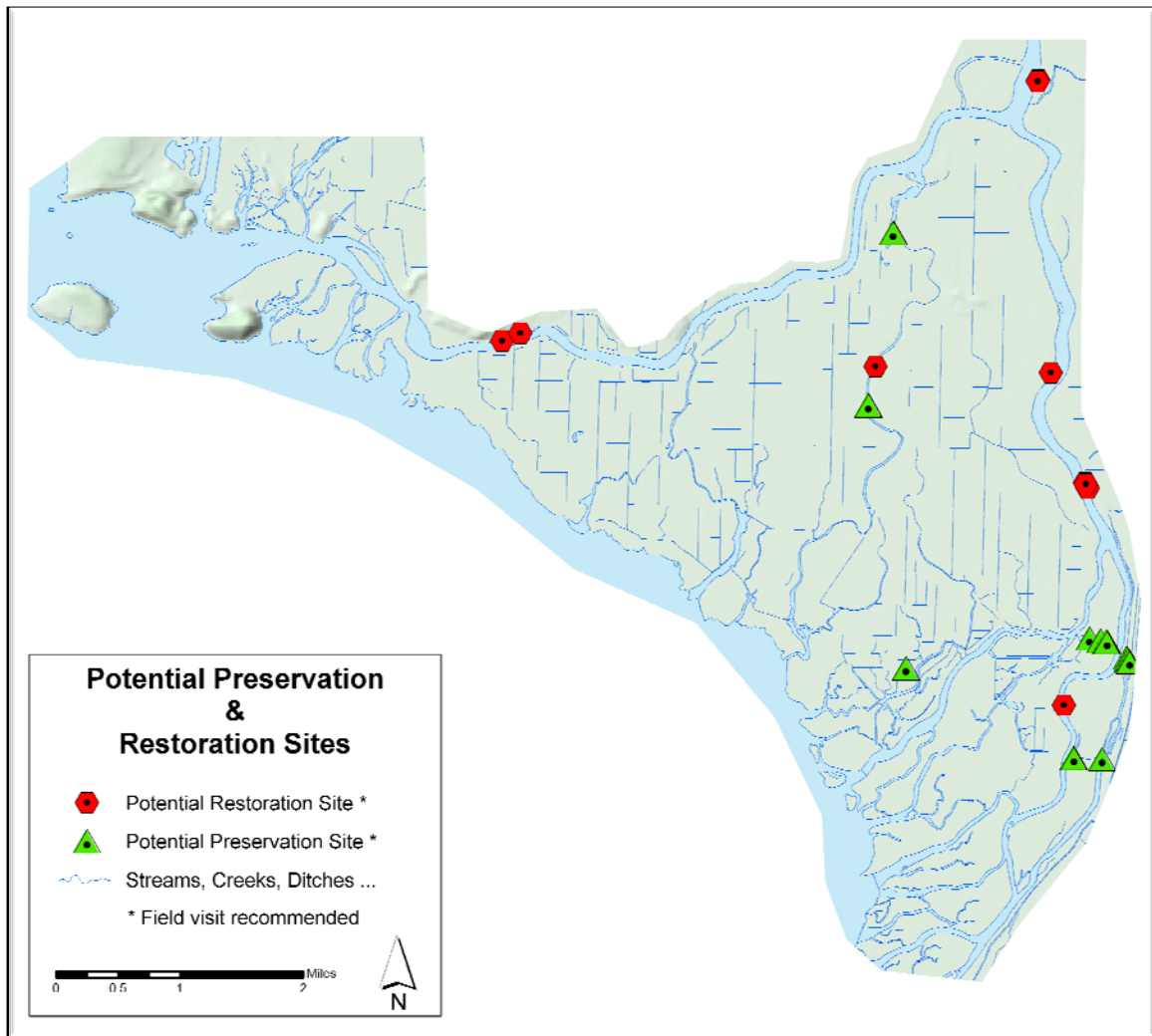


Once the primary combined ranking was complete, the secondary riparian characteristics regarding forest buffer width and percent conifer forested were used to more specifically identify those sites (RCSs) that might be good candidates for restoration and/or preservation activities based on their overall riparian condition. It should be emphasized that all sites identified by this model for preservation or restoration activities should be verified via assessment in the field. I did not perform field assessments on the selected

preservation and restoration sites due to right of entry issues on private property and limited access to some sites.

The sites identified for preservation and restoration are shown in Figure 4.7.

Figure 4.7 Potential preservation and restoration sites for which field visits are recommended.



The process for identifying the sites that may be in the most need of preservation efforts was as follows: Of the 511 RCSs having a PCR value of 3 or “good,” 182 had at least 40% of the 30-meter riparian buffer forested on at least one side of the RCS. Of those, 15 RCSs had

riparian buffers consisting of a minimum of 40% conifer-dominated forest on at least one side of the RCS and were not coded as shoreline segments in the hydrology dataset.

Shoreline segments are those open to Skagit Bay to the west of the study area.

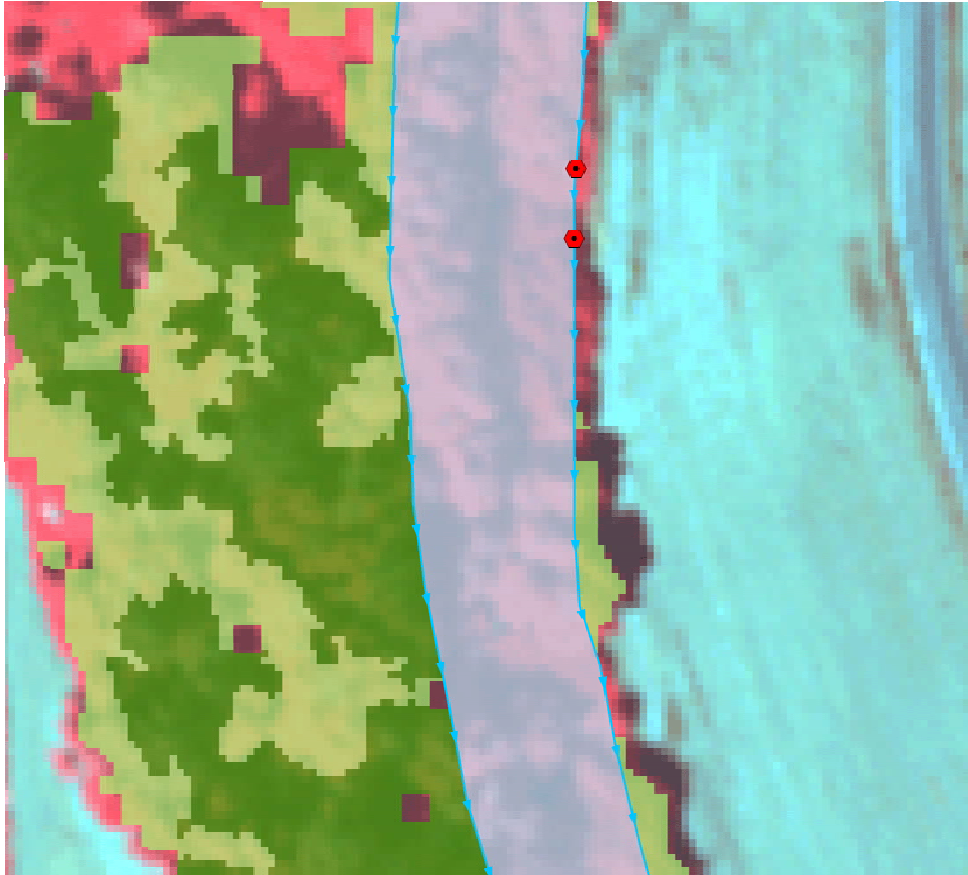
The procedure for identifying those sites that might be in the most need of restoration activities was more involved than identifying preservation sites due to such a larger number of RCSs that received a PCR value of 1 or “poor.” First, all RCSs with an LWD Index of zero, a Shade Index of zero, a Forest Buffer Width Rank of 1 and a Percent Conifer Rank of 1. Of those, I selected only RCSs where both sides resulted in a forested buffer width of zero. Next I selected only those where both sides contained no conifer-dominant forest whatsoever. Using the LWD MSAHT and shade MSAHT frequency values, I selected 18 potential restoration sites within the study area (Figure 4.8). It should be noted that some sites appear to be stacked upon each other when viewed at the scale shown in Figure 4.8. However, Figure 4.9 shows a series of consecutive RCSs that the model identified as potential preservation sites at a larger scale. These consecutive sites appear as a single green triangle in Figure 4.8.

Figure 4.8 A series of RCSs are identified here as potential preservation sites with green triangles overlaid to identify them. Conifer-dominant forest patches in dark green and deciduous-dominant forest patches shown in light green. RCSs along each side of the stream are shown as blue 10-meter segments with arrows signifying each segment's endpoint.



Likewise, Figure 4.10 shows two consecutive RCSs identified as potential preservation sites. These consecutive sites appear as a single red point in Figure 4.9.

Figure 4.9 Two RCSs are identified here as potential restoration sites with red points overlaid to identify them. Conifer-dominant forest patches in dark green and deciduous-dominant forest patches shown in light green. RCSs along each side of the stream are shown as blue 10-meter segments with arrows signifying each segment's endpoint.



#### 4.7 Future Model Improvements

The model I developed for this research was designed to evaluate the study area by focusing on two primary riparian zone functions as they impact salmon habitat, potential large woody debris recruitment and potential shade production. The model also provides information about two secondary riparian area characteristics, forest buffer width and species composition. I recognize, however, that numerous other parameters exist that

significantly impact riparian zones and their ability to support healthy salmon habitat. I look forward to continuing modification of this model so that it may improve over time by incorporating more of these variables. One such parameter is the evaluation of LWD efficiency. Currently, the model considers actual tree height versus a maximum study area height tree which provides some indication of the size of the LWD potentially contributed to a stream in terms of piece length. However, it does not account for the diameter of a piece that may be contributed and thus the addition of an estimate of the maximum diameter of a potential LWD piece contributed would be an improvement. Additionally, the model does not account for forest density which can have a significant impact on shade production by a riparian forest. Thus, modifying the model to consider forest density would definitely be an improvement. I would also like to see the model improved by accounting for ground slope so that a potential LWD piece might be weighted with a higher or lower probability of reaching a watercourse due to the direction of ground slope upon which it is located. Furthermore, it may be necessary to consider the proximity of an RCS to urbanized areas, road features and the like when evaluating it as a potential restoration or preservation site since decision-makers will likely want to get the most of every dollar spent towards preservation and/or restoration. All primary ecological factors being equal, further limiting preservation or restoration sites based on these types of criteria may make a significant difference with regard to the quantity of sites that can potentially receive funding for preservation or restoration activities.

## 5.0 Conclusions

The Puget Sound region has become a focal point for various parties of interest involved in the selection, development and maintenance of salmon habitat preservation and restoration activities within its riparian areas. Anthropogenic impacts have dramatically degraded riparian areas which in turn has degraded aquatic habitat by altering both the amount of LWD and shade that riparian forests can provide. Given the uniqueness of each riparian forest and the needs of various organizations to assess and monitor their function, it is important to develop tools that can aid the decision-making process by analyzing and mapping riparian forest conditions and function.

The purpose of this study was to develop a GIS model that focuses primarily on LWD recruitment potential and shade potential along with other secondary riparian forest characteristics to provide the user with a tool for remotely assessing and monitoring riparian areas as they pertain to salmon habitat. While the intent of the study was to provide a way to use remotely sensed data (lidar and color imagery) to develop the primary model inputs rather than field surveys, it should be noted that field assessment of all selected sites should be always be diligently performed to be certain which sites in fact require restoration or preservation. However, the results of this study can be applied to dramatically reduce the amount of time and resources spent on field assessments.

The study area for this research was located in the southwestern coastal region of Skagit County, Washington where land-use is primarily agricultural in nature. The entire study area consisted of 40,341 sites (10-meter segments) along 403 kilometers of watercourse. Of those, 15 were identified as primary targets for preservation and 18 were

identified as primary restoration sites. Since the bulk of the study area is in the agricultural zone, the farming community will play a critical role in any restoration and/or preservation efforts.

It is vital to note that although this study focused on a primarily agricultural study area, degradation of aquatic habitat in Skagit County is not solely due to the deterioration of riparian forest. The decreased quality of local salmon habitat is also impacted by years of hydrologic modification, failure to maintain adequate stream flow and water quality as well.

The farming community of Skagit County as well as numerous other parties of interest that include federal, state, tribal and local government agencies have all taken part in some form of various restoration and preservation efforts within the county. These efforts continue today despite litigation and often heated debates since all parties involved, but especially farmers, have vested and often emotional interests in how restoration and preservation activities occur. Regardless of the shape that riparian restoration strategies may take, hopefully this research was able to provide a tool that can be objectively applied so that all parties involved can utilize the information provided to make the best informed decisions when it comes to restoration and preservation planning efforts within Skagit County.

## Literature Cited

- Adams, T.A., and K. Sullivan. 1990. The physics of forest stream heating: a simple model. Timber-Fish-Wildlife Report No. TFW-WQ3-90-007, Washington Department of Natural Resources. Olympia, Washington.
- Barton, D.R., W.D. Taylor, and R.M. Biette. 1985. Dimensions of riparian buffer strips required to maintain trout habitat in southern Ontario streams. *North American Journal of Fisheries Management*. 5:364-378.
- Beechie, T.J., G. Pess, P. Kennard, R.E. Bilby, S. Bolton, 2000. Modeling recovery rates and pathways for woody debris recruitment in northwestern Washington streams. *North American Journal of Fisheries Management*. 20:436-452.
- Beechie, T.J., and Sibley, T.H. 1997. Relationships between channel characteristics, woody debris, and fish habitat in northwestern Washington streams. *Transactions of the American Fisheries Society*. 126:217-229.
- Beechie, T.J. 1998 Rates and pathways of recovery for sediment supply and woody debris recruitment in northwestern Washington streams, and implications for salmonid habitat restoration. Doctoral dissertation, University of Washington. Seattle, Washington.
- Berg D.R., A. McKee, and M.J. Maki. 2002. Restoring floodplain forests. Successional dynamics in forest riparian zones. Pgs. 243-285 in D.R. Montgomery, S. Bolton, D.R. Booth, L.Wall, editors. *Restoration of Puget Sound Rivers*. University of Washington, center for Water and Watershed Studies.
- Beschta, R.L., R.E. Bilby, G.W. Brown, L.B. Holtby, and T.D. Hofstra. 1987. Stream temperature and aquatic habitat: fisheries and forestry interactions. *Streamside Management: Forestry and Fishery Interaction*. Seattle, Washington, University of Washington, College of Forest Research, pgs. 191-232.
- Bilby, R.E. and J.W. Ward. 1989. Changes in characteristics and function of woody debris with increasing size of streams in western Washington. *Transactions of the American Fisheries Society*. 118:368-378.
- Bisson, P.A., R.E. Bilby, M.D. Bryant, C.A. Dolloff, G.B. Greete, R.A. House, M.L. Murphy, K.V. Koski, and J.R. Sedell. 1987. Large Woody Debris in forested Streams in The Pacific Northwest: Past, Present, and Future. *Streamside Management: Forestry and Fishery Interactions*. University of Washington, College of Forest Research: pgs. 143-193. Contribution No. 57. Seattle, Washington.

- Brazier, J.R. and G.W. Brown. 1973. Buffer strips for stream temperature control. Research Paper No. 15, Forest Research Laboratory, Oregon State University, Corvallis, Oregon.
- Brown, G.W. 1969. Predicting temperatures of small streams. *Water Resources Research*. 5(1):68-75.
- Brown, G.W. and J.T. Krygier. 1970. Effects of clear cutting on stream temperature. *Water Resources Research*. 6:1133-1139.
- Bryant, M.D. 1983. The role and management of woody debris in west coast salmonid nursery streams. *North American Journal of Fisheries Management*. 3:322-330.
- Campbell, James B. 1996. *Introduction to Remote Sensing*. The Guilford Press, New York.
- Castelle, A.J., Johnson, A.W., and Conolly, C. 1994. Wetland and stream buffer size requirements - a review. *Journal of Environmental Quality*. 23:878-882.
- Congalton, Russell G., Kevin Birch, Rick Jones and James Schriever. 2002. Evaluating remotely sensed techniques for mapping riparian vegetation. *Computers and Electronics in Agriculture* 37(2002):113-126.
- Cross, J. 2002. Measuring the impact of harvest intensity on riparian forest functionality in terms of shade production and large woody debris recruitment potential: two models. Masters thesis, University of Washington. Seattle, Washington.
- Duncan, S.H., R.E. Bilby, J.W. Ward, and J.T. Heffner. 1987. Transport of Road-surface sediment through ephemeral stream channels. *Water Resources Bulletin* 23:113-119.
- Endreny, Theodore A.. 2002. Forest buffer strips: Mapping the water quality benefits. *Journal of Forestry*, 100(1): 35-40.
- Gregory, S.V., F.J. Swanson, A. McKee, and K.W. Cummins. 1991. An ecosystem perspective of riparian zones. *Bioscience* 41(8): 540-551.
- Hyatt, T.L., T.Z. Waldo, and T.J. Beechie. 2004. A watershed scale assessment of riparian forests, with implications for restoration. *Restoration Ecology* 12(2):175-183.
- Keller, E.A., and F.J. Swanson. 1979. Effects of Large Organic Material on Channel Form and Fluvial Processes. *Earth Surface Process Landforms* 4:361-380.
- King County. 1997. The value of riparian vegetation.  
<http://dnr.metrokc.gov/wlr/pi/ripveg.htm>
- Lamberti, G.A., S.V. Gregory, L.R. Ashkenas, R.C. Wildman, and K.M.S. Moore. 1991.

Stream ecosystem recovery following a catastrophic debris flow. *Canadian Journal of Fisheries and Aquatic Science* 48:196-208.

Lunetta, R.S., B.L. Cosentino, D.R. Montgomery, E.M. Beamer and T.J. Beechie. 1997. GIS-Based Evaluation of Salmon Habitat in the Pacific Northwest. *Photogrammetric Engineering and Remote Sensing* 63(10):1219-1229.

Murgatroyd, A.L. and J.L. Ternan. 1983. The impact of afforestation on stream bank erosion and channel form. *Earth Surface Process and Landforms* 8:357-369.

Naiman, R.J., T.J. Beechie, L.E. Benda, D.R. Berg, P.A. Bisson, L.H. MacDonald, M.D. O'Connor, P.L. Olson, and E.A. Steel. 1992. Fundamental elements of ecologically healthy watersheds in the Pacific Northwest coastal ecoregion, in Naiman, R.J. (editor) *Watershed Management*, pp. 127-188.

Parkyn, S.M., R.J. Davies-Colley, N.J. Halliday, K.J. Costley, and G.F. Croker. 2003. Planted riparian buffer zones in New Zealand: Do they live up to expectations? *Restoration Ecology* 11(4): 436-447.

Robison, E.G., and R.L. Beschta. 1990. Identifying trees in riparian areas that can provide coarse woody debris to streams. *Forest Science* 36:790-801.

Sedell, J.R., P.A. Bison, F.J. Swanson, and S.V. Gregory. 1988. What We Know About Large Trees that Fall into Streams and Rivers. In: C. Maser. *From the Forest to the Sea: A Story of Fallen Trees*. Pgs. 47-81. General Technical Report PNW-GTR-229. USDA Forest Service, Pacific Northwest Research Station. Portland, Oregon.  
URL: <http://www.fs.fed.us/pnw/pubs/229chpt3.pdf>

Skagit County. 2003. Skagit County Critical Areas Ordinance.  
[http://www.skagitcounty.net/PlanningAndPermit/Documents/Code/title14/Ch14\\_24.pdf](http://www.skagitcounty.net/PlanningAndPermit/Documents/Code/title14/Ch14_24.pdf)

Sovell, L.A., B. Vondracek, J.A. Frost, and K.G. Mumford. 2000. Impacts of rotational grazing and riparian buffers on physicochemical and biological characteristics of southeastern Minnesota, USA, streams. *Environmental Management* 36(6):629-641.

Sullivan, K., J. Tooley, K. Doughty, J.E. Caldwell, and P. Knudsen. 1990. Evaluation of prediction models and characterization of stream temperature regimes in Washington. TFW-WQ3-90-006. Olympia, Washington.

Swanson, F.J., Lienkaemper, W.L., and Sedell, J.R. 1976. History, physical effects, and management implications of large organic debris in western Oregon streams. General Technical Report PNW-56. USDA Forest Service, Pacific Northwest Research Station. Portland, Oregon.

Turner, M.G., R.H. Gardner, and R.V. O'Neill. 2001. *Landscape Ecology in Theory and*

Practice. Springer-Verlag, New York, pp. 272-280.

U.S. Naval Observatory, Astronomical Applications Department. 2006. Sun or Moon Altitude/Azimuth Table for One Day <http://aa.usno.navy.mil/data/docs/AltAz.html>

Vannote, R.L., G.W. Minshall, K.W. Cummins, J.R. Sedell, and C.E. Cushing. 1980. The River Continuum Concept. *Canadian Journal of Fisheries and Aquatic Sciences* 37:130-137.

Waldo, T.Z. 2003. A GIS strategy for riparian restoration of salmon habitat in the Nooksack River basin. Masters thesis, Western Washington University. Bellingham, Washington.

Washington Forest Practices Board (WFPB). 1997. Washington Forest Practices Board manual: standard methodology for conducting watershed analysis under 222-22 WAC Version 4.0. Washington Department of Natural Resources, Forest Practices Division, Olympia, WA.

Washington State Department of Natural Resources, Forest Practices Division. April 2001. Final Environmental Impact Statement. Olympia, WA.  
URL: [www.dnr.wa.gov/forestpractices/eis](http://www.dnr.wa.gov/forestpractices/eis).

Young, K.A. 2000. Riparian zone management in the pacific northwest: Who's cutting what? *Environmental Management* 26(2): 131-144.

Zwienicki, M.A. and M. Newton. 1999. Influence of streamside cover and stream features on temperature trends in forested streams of western Oregon. *Western Journal of Applied Forestry* 14(2):106-113.